# 3nm Multi-Narrowband Filter Comparison

by Jim Thompson, P.Eng
Test Report – October 31st, 2022

**Introduction:**
The performance of multi-narrowband filters (i.e. filters with two to four narrow pass bands located at key nebula emission wavelengths) continues to be improved by filter manufacturers. Where six months ago the narrowest filter pass bands one could buy was 5nm (the Antlia ALP-T), now there are two new filters on the market with pass bands only 3nm wide. This test report compares the performance of these two new filters to existing multi-narrowband filters with the objective of evaluating the magnitude of the performance increase one can realize by using filters as narrow as 3nm.

**Objective:**
The objective of this test report is to evaluate the performance of the Optolong L-uLtimate and Askar Colour Magic Duo-Narrowband filters, comparing them to each other and to other multi-narrowband filters already on the market. The list of filters considered in this test report is as follows:

- Radian Triad Ultra – 5nm/4nm/4nm/4nm wide bands, $1075USD
- Optolong L-eXtreme – 7nm/7nm wide bands, $309USD
- Antlia ALP-T – 5nm/5nm wide bands, $380USD
- Askar Colour Magic Duo-Narrowband – 3nm/3nm wide bands, $539USD
- Optolong L-uLtimate – 3nm/3nm wide bands, $389USD

I have procured by various means a sample of all the filters in this list. If theory is born out in the test results, there should be an observable improvement in deepsky object contrast as I move down the list of filters since they have progressively narrower pass bands. Filter performance was evaluated during this test based on the increase in contrast between the observed object and the background, which is a measurable quantity. It was evaluated quantitatively using the measured filter spectra combined with the spectra of several common deepsky objects, and by direct measurement from images captured using each filter and a one-shot colour (OSC) camera. The image data was also used to evaluate the signal-to-noise ratio (SNR) achieved using each filter.

**Method:**
Testing consisted of data collection from the following sources:

- Spectral transmissivity data, from near-UV to near-IR, measured using an Ocean Optics USB4000 spectrometer; and
- Image data, collected using a ZWO ASI533MC Pro OSC camera, and one of three different telescopes:
    - Mallincam VRC-10” Ritchey-Chretien + Astrophysics 0.67x focal reducer, effective f/6.5;
    - William Optics FLT98 triplet apochromatic refractor, native f/6.3; or
    - Askar FMA230 quad apochromatic refractor, native f/4.5.

The spectrometer data was collected in my basement workshop with the USB4000 and a broad spectrum light source. Filter spectrums were measured for a range of filter angles relative to the light path, from 0° (perpendicular) to 20° off-axis. The spectrometer was recently upgraded, replacing the entrance slit and diffraction grating, to give a wavelength resolution of 0.5nm.

The image data was collected from my backyard in central Ottawa, Canada where the naked eye limiting magnitude (NELM) due to light pollution is +2.9 on average (Bortle 9+). I switched filter configurations using a ZWO 2" filter drawer. Each time I changed filters I refocused on a conveniently located bright star using a Bahtinov mask. Images with the various filters under test were collected with the scopes at their native focal ratios with the exception of the RC: f/6.5 for the VRC10, f/6.3 for the FLT98, and f/4.5 for the FMA230. Images of four different deepsky objects were captured, each on a different evening as follows:

1. Entire Veil Nebula (Cygnus Loop), September 8th, using FMA230
2. M27 Dumbbell Nebula, September 29th, using VRC10
3. NGC6960 Western Veil Nebula, October 18th, using FLT98
4. M42 Orion Nebula, October 22nd, using FLT98

The purpose of selecting different deepsky objects was to use the filters on targets with varying amounts of H-α and O-III emission. The Moon had an impact on the first imaging night, it being 2 days before the full Moon. The Moon was either not up or not bright enough to have an impact on the other imaging sessions. The first, second, and fourth imaging sessions used sub-exposure times that varied according to the narrowness of the filter pass bands so that the overall image exposure (brightness) as captured was roughly the same. The third imaging session used a fixed sub-exposure time of 60s for all filters to allow for a more direct comparison of SNR. All images from the first session are live stacks of 10 minutes total duration, captured using Sharpcap in 16-bit FITS format. Images from the other three sessions were stacks of 5 minutes total duration. Note that the sample of the Askar filter did not arrive until the beginning of October, so image data was collected with that filter only during the last two sessions.

**Results – Spectrum Measurements:**

Using the test method mentioned above the spectral transmissivity for each filter was measured for a range of filter angles relative to the light path. Figure 1 presents a plot of the resulting spectral transmissivity data for the case of the filter perpendicular to the light path. Both of the 3nm filters have their O-III pass band center wavelengths (CWL) well positioned over 500.7nm. The Askar filter's H-α pass band CWL is well centered on 656.3nm, but the L-uLtimate filter's H-α band CWL is shifted slightly to the right which should improve performance at faster f-ratios. Although advertised to have the same full width half maximum (FWHM) band width, the Askar filter was measured to have significantly wider pass bands than the L-uLtimate filter. Peak transmissivity values in each band are comparable between the two 3nm filters. Discussion of the results for the other filters under test has already been presented in my June 2022 test report: "ALP-T Comparison Test".

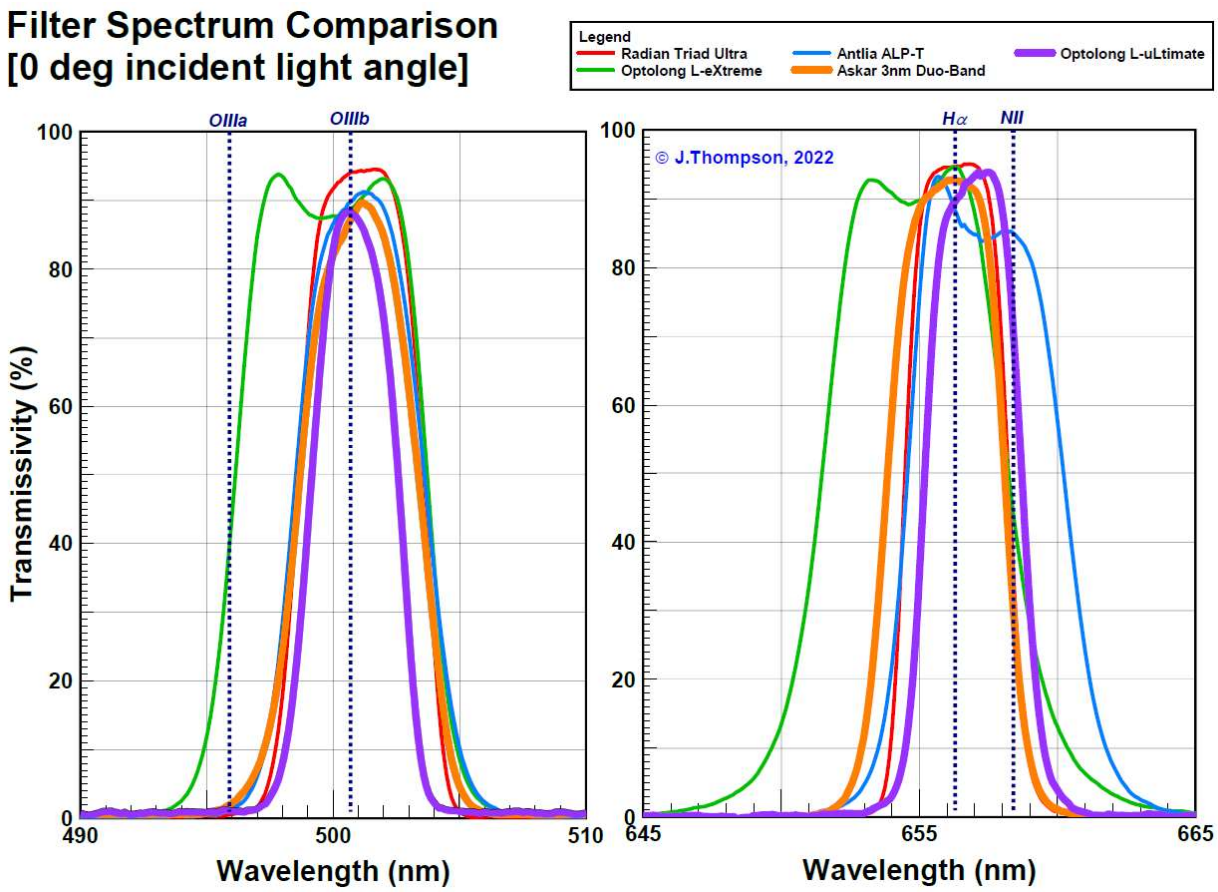


**Figure 1 Measured Spectral Response of Tested Filters – Filter Perpendicular to Light Path**

The impact of angle on each filter's respective emission band transmission is shown in Figure 2 for the O-III and H-α bands. In general, filters with wider pass bands were less sensitive to angle than filters with narrow pass bands. There was however a significant amount of variation due to the combination of FWHM and CWL; filters that have their bands shifted to the left perform more poorly than those with bands shifted to the right. As a result of this, the Askar filter has lower sensitivity to angle for the O-III band than the L-uLtimate, but worse sensitivity to angle for the H-α band.

Figure 2 also has black vertical lines representing different optics f-ratios. These lines are positioned at the angle values corresponding to light coming from the outer edge of the scope's aperture for the noted f-ratio. For example: for an f/2 scope the light from the outer edge of the optics is passing through the filter at a 14° angle. The net performance of a filter on any particular speed of optics is an area weighted average of the filter's performance, from the center of the optics (perpendicular light path) out to the edge of the aperture (max light path angle). Using the measured filter spectra at each angle I have calculated a net filter spectrum for a selection of telescope f-ratios. The area averaging process is illustrated in Figure 3. Essentially the aperture of the scope is divided into rings defined by the angles at which I have measured filter data. The percentage each ring is of the total primary optical area is the weighting applied to that particular spectrum in the average. Figures 4 through 7 present the resulting net spectra

for the different speeds of telescope. The shift in filter response between that shown in Figure 1 and for the f/6.3 telescope (Figure 4) is almost zero, but is very significant for the f/2 scope (Figure 7). The effects of filter band shift are worse on the Hyperstar scope due to the large central obstruction which results in a larger percentage of the light having to pass through the filter at an angle.

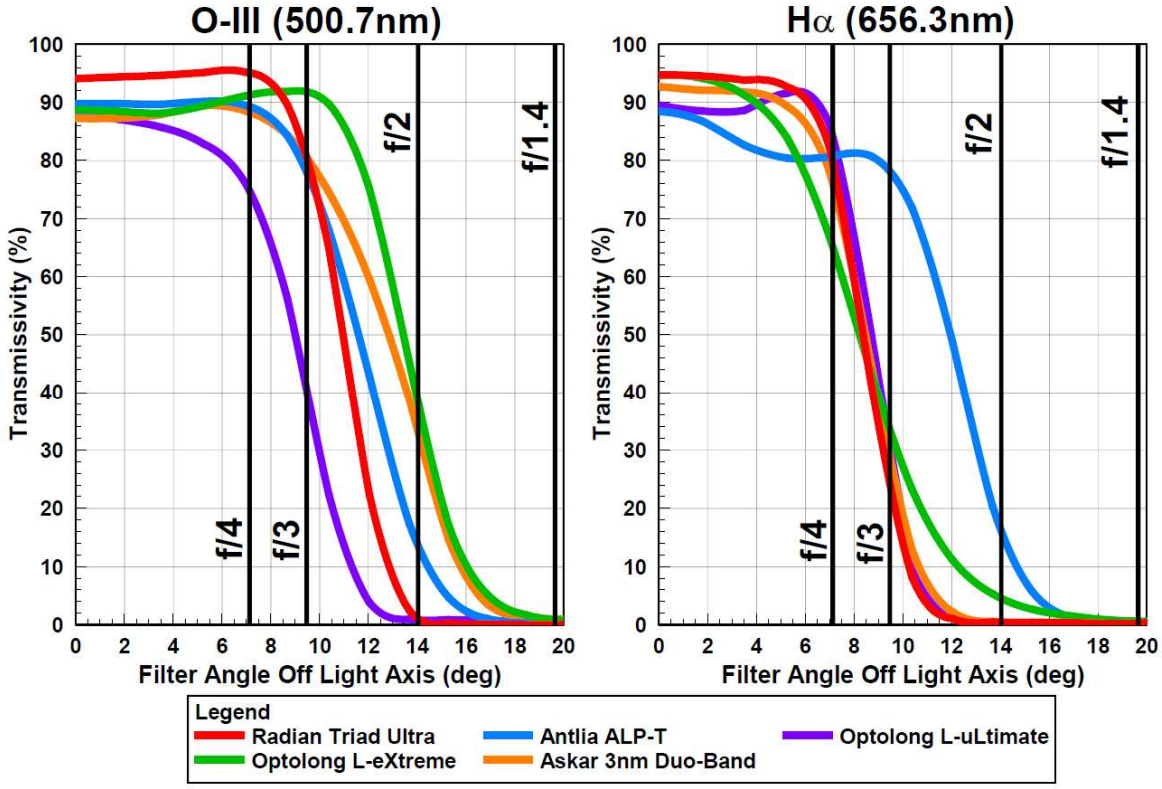


**Figure 2 Measured Impact of Angle on Filter Response**

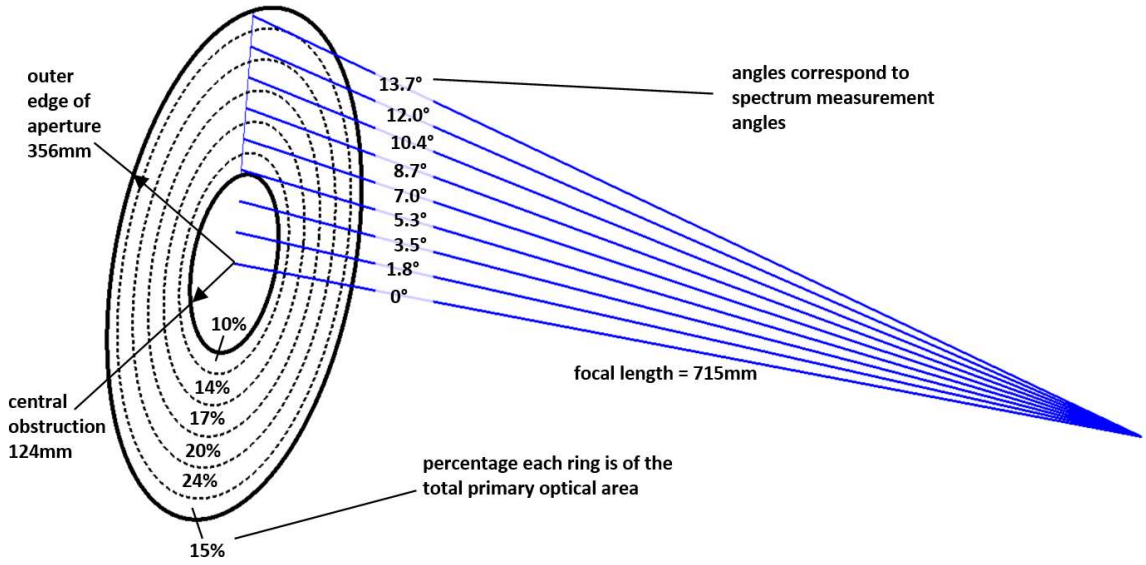


**Figure 3 Illustration of Area Weighted Average Filter Response Calculation – C14 Hyperstar**

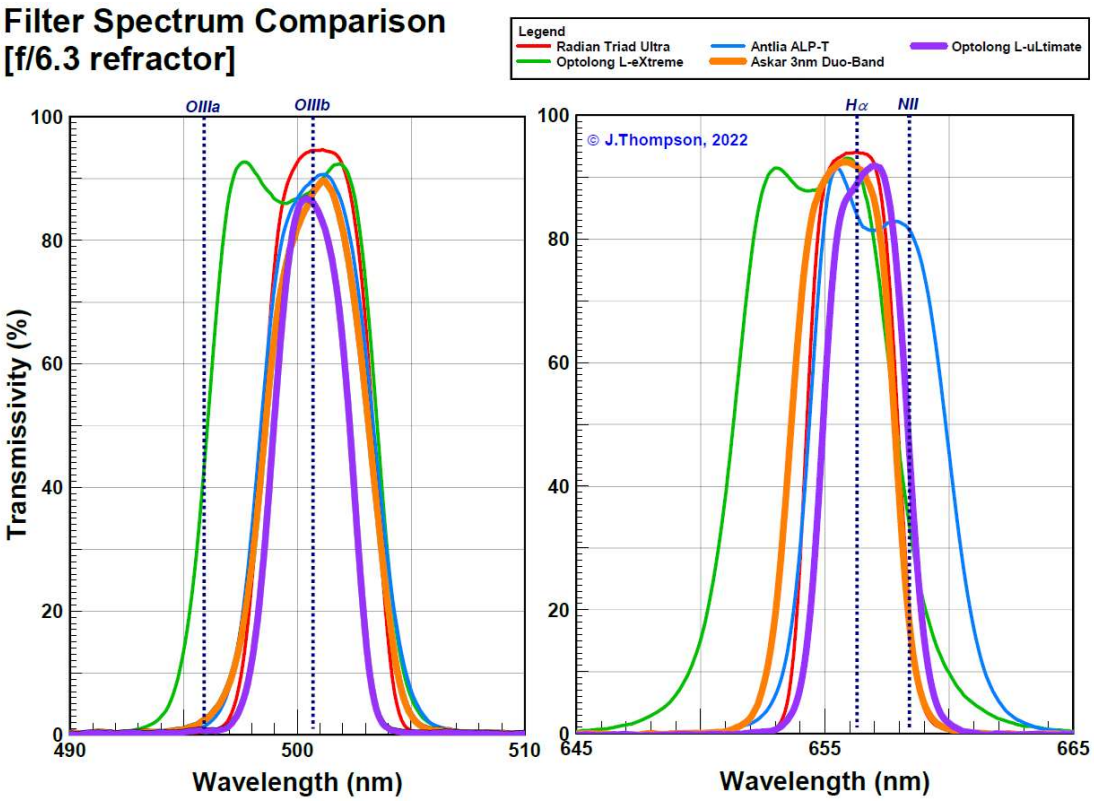


**Figure 4 Net Spectral Response of Tested Filters – f/6.3 Refractor Area Weighted Average**

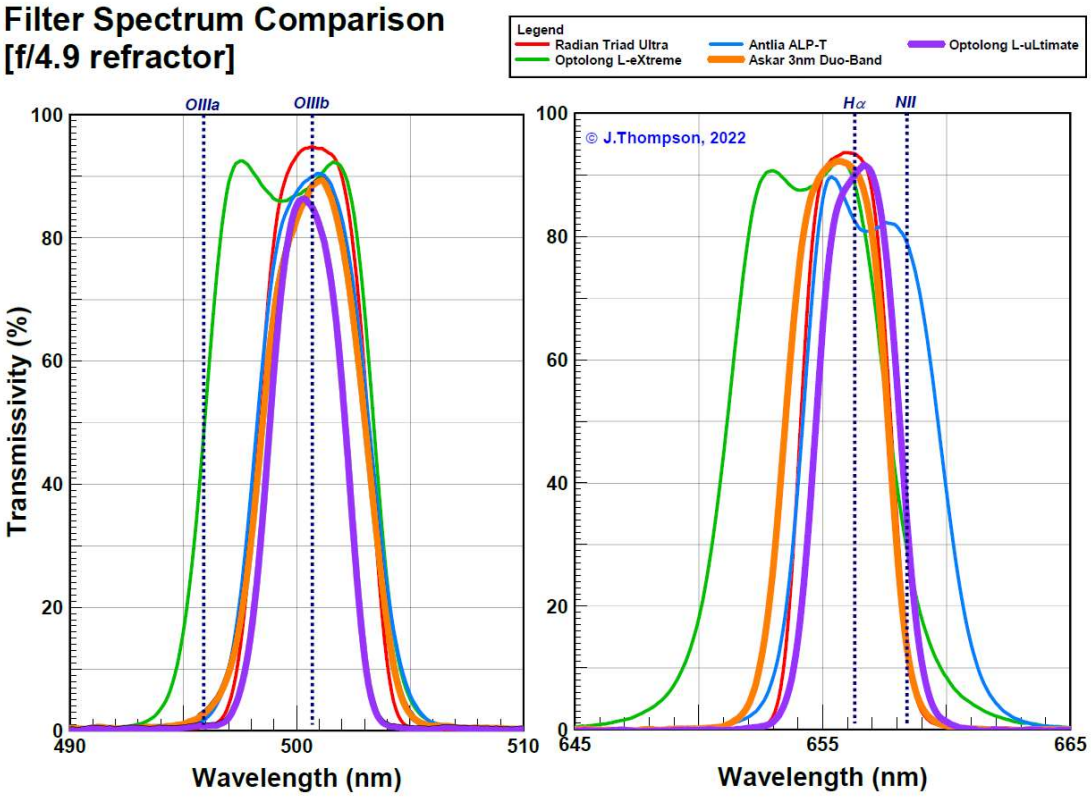


**Figure 5 Net Spectral Response of Tested Filters – f/4.9 Refractor Area Weighted Average**

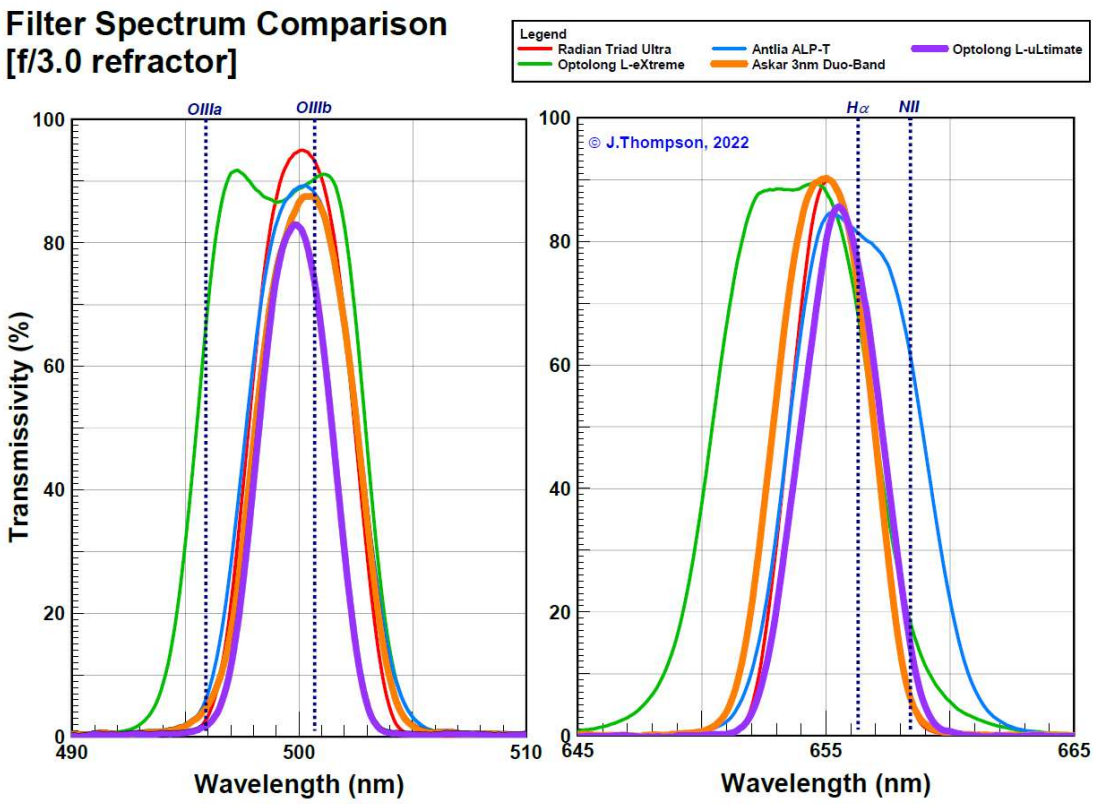


**Figure 6 Net Spectral Response of Tested Filters – f/3.0 Refractor Area Weighted Average**

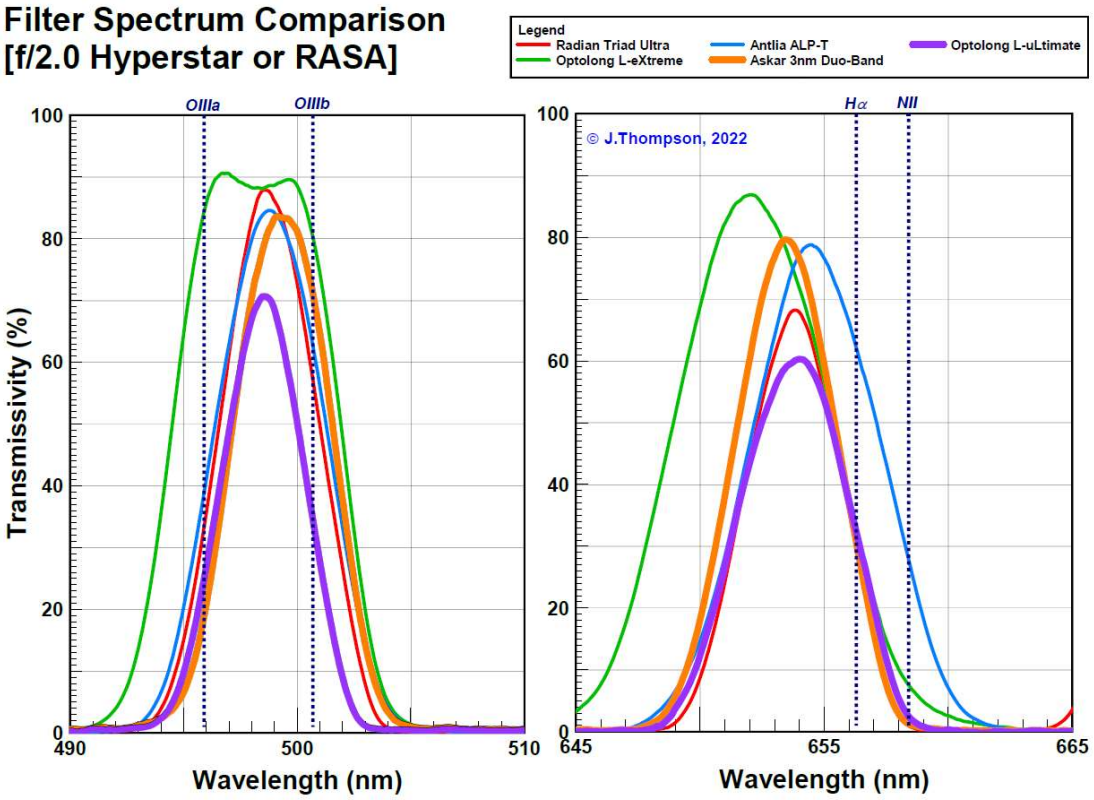


**Figure 7 Net Spectral Response of Tested Filters – f/2 C14 w/Hyperstar Area Weighted Average**

With the net filter spectra in hand, it was possible to extract overall performance related statistics for each filter, such as transmission values at key wavelengths of interest and pass band widths. These filter statistics are provided in Table 1, including a calculated value for percent Luminous Transmissivity (%LT), a single number that describes generally how much light is getting through the filter. The calculated value of %LT depends on the spectral response of the detector, which in this case is assumed to be a modern back illuminated CMOS sensor. I have included transmission measurements in the table for a range of telescope f-ratios, from f/∞ (perfectly parallel & perpendicular light) down to f/2. Included in the table are the filter statistics quoted by the manufacturers.

| Filter | Scope Optics | %LT* | Hbeta/O-III Pass Band | | | | Halpha Pass Band | | | |
|---|---|---|---|---|---|---|---|---|---|---|
| | | | FWHM | Hbeta (486.1) | O-IIIA (495.9) | O-IIIB (500.7) | FWHM | Halpha (656.3) | N-II (658.4) | S-II (672.4) |
| Radian Triad Ultra | *manuf.* | - | *5/4nm* | *79%* | - | *97%* | *4/4nm* | *87%* | - | *90%* |
| | f/∞ | 3.9% | 4.8/4.8nm | 90.3% | 0.5% | 94.1% | 3.5/4.1nm | 94.7% | 35.9% | 95.6% |
| | f/6.3** | 3.8% | 4.8/4.7nm | 84.7% | 0.5% | 94.6% | 3.5/4.0nm | 94.0% | 20.3% | 94.8% |
| | f/4.9** | 3.8% | 4.7/4.7nm | 79.1% | 0.6% | 94.8% | 3.5/4.0nm | 93.5% | 14.4% | 94.5% |
| | f/3.0** | 3.7% | 4.7/4.6nm | 49.6% | 2.6% | 93.2% | 3.5/4.0nm | 74.1% | 6.1% | 81.7% |
| | f/2*** | 3.6% | 4.8/4.7nm | 17.1% | 32.7% | 57.0% | 4.3/4.7nm | 30.0% | 1.0% | 36.6% |
| Optolong L-eXtreme | *manuf.* | - | *7nm* | *0%* | - | *>90%* | *7nm* | *>90%* | - | *0%* |
| | f/∞ | 3.2% | 7.5nm | 0% | 38.7% | 88.7% | 6.6nm | 94.6% | 44.2% | 0% |
| | f/6.3 | 3.1% | 7.4nm | 0% | 42.0% | 88.3% | 6.5nm | 91.8% | 33.9% | 0% |
| | f/4.9 | 3.1% | 7.4nm | 0.1% | 47.0% | 88.8% | 6.5nm | 88.6% | 29.3% | 0% |
| | f/3.0 | 3.1% | 7.4nm | 0.1% | 65.5% | 90.4% | 6.7nm | 68.3% | 18.4% | 0% |
| | f/2 | 3.1% | 7.6nm | 0.1% | 84.0% | 80.2% | 6.9nm | 33.4% | 7.6% | 0% |
| Antlia ALP-T | *manuf.* | - | *5nm* | *0%* | - | *82%* | *5nm* | *90%* | - | *0%* |
| | f/∞ | 2.3% | 5.1nm | 0% | 1.1% | 89.8% | 5.5nm | 88.4% | 85.0% | 0% |
| | f/6.3 | 2.2% | 4.9nm | 0% | 1.3% | 89.7% | 5.4nm | 83.9% | 81.4% | 0% |
| | f/4.9 | 2.2% | 4.9nm | 0% | 1.6% | 89.9% | 5.5nm | 82.5% | 79.0% | 0% |
| | f/3.0 | 2.2% | 5.0nm | 0% | 5.8% | 88.0% | 5.6nm | 81.4% | 61.6% | 0% |
| | f/2 | 2.2% | 5.3nm | 0% | 38.3% | 62.5% | 5.9nm | 62.3% | 28.0% | 0% |
| Askar Colour Magic 3nm Duo-Narrowband | *manuf.* | - | *3nm* | *0%* | - | *85%* | *3nm* | *88%* | - | *0%* |
| | f/∞ | 1.9% | 4.7nm | 0% | 1.9% | 87.2% | 4.1nm | 92.7% | 30.4% | 0% |
| | f/6.3 | 1.9% | 4.6nm | 0% | 2.3% | 87.8% | 4.0nm | 91.7% | 17.9% | 0% |
| | f/4.9 | 1.9% | 4.6nm | 0% | 2.7% | 88.4% | 4.0nm | 90.8% | 13.4% | 0% |
| | f/3.0 | 1.9% | 4.6nm | 0% | 4.6% | 87.2% | 4.1nm | 72.8% | 6.2% | 0% |
| | f/2 | 1.9% | 4.7nm | 0% | 18.5% | 70.8% | 4.6nm | 30.8% | 1.3% | 0% |
| Optolong L-uLtimate | *manuf.* | - | *3nm* | *0%* | - | *90%* | *3nm* | *88%* | - | *0%* |
| | f/∞ | 1.5% | 3.4nm | 0% | 1.0% | 88.2% | 3.3nm | 89.6% | 71.2% | 0% |
| | f/6.3 | 1.4% | 3.3nm | 0% | 0.6% | 86.0% | 3.3nm | 88.8% | 45.9% | 0% |
| | f/4.9 | 1.4% | 3.3nm | 0% | 0.7% | 84.8% | 3.3nm | 89.9% | 34.2% | 0% |
| | f/3.0 | 1.4% | 3.4nm | 0% | 1.6% | 73.2% | 3.5nm | 76.5% | 14.8% | 0% |
| | f/2 | 1.4% | 4.0nm | 0% | 24.5% | 34.1% | 5.0nm | 32.5% | 2.5% | 0% |

* calculated assuming spectral QE curve for IMX174M with no UV/IR blocking filter; ** refractor; *** C14 w/Hyperstar

**Table 1 Measured Filter Performance Summary**

Knowing the measured spectral response of the sample filters also allowed me to predict the theoretical relative performance of each filter when imaging an emission nebula. To do this I used the method I developed back in 2012 which applies the spectral response of the filter and sensor combined with the spectral emission from the deepsky object and background light polluted sky to estimate the apparent luminance observed. To help visualize the results of this analysis I have plotted the predicted % increase in contrast (vs. no filter) for each filter versus the filter's %LT. Figure 8 shows the resulting plot corresponding to filter performance when using a

OSC CMOS camera under heavily light polluted skies, Bortle 9+ (i.e. same as my backyard). Note that these are theoretical predictions of the increase in visible contrast between the object and the background. The absolute values of my predictions may not reflect what a user will experience with their own setup, but the predicted relative performance of one filter to another should be representative. In general, the desired performance for a filter is high contrast increase and high %LT, so the higher and more to the right a filter's performance is in the plot the better. Each filter's performance is plotted as a short line to show how the performance is predicted to change depending on the f-ratio of the telescope you are using the filter with. Slow f-ratio optics are at the right-most end of the line, f/3 is roughly in the middle of the line, and f/2 is at the left-most end of the line. I have plotted predicted filter performance for two different types of nebulae: bright O-III rich like M27 the Dumbbell Nebula (thinner line w/ triangle data markers), and faint H-α rich like NGC7000 the North American Nebula (thicker line w/ circle data markers).

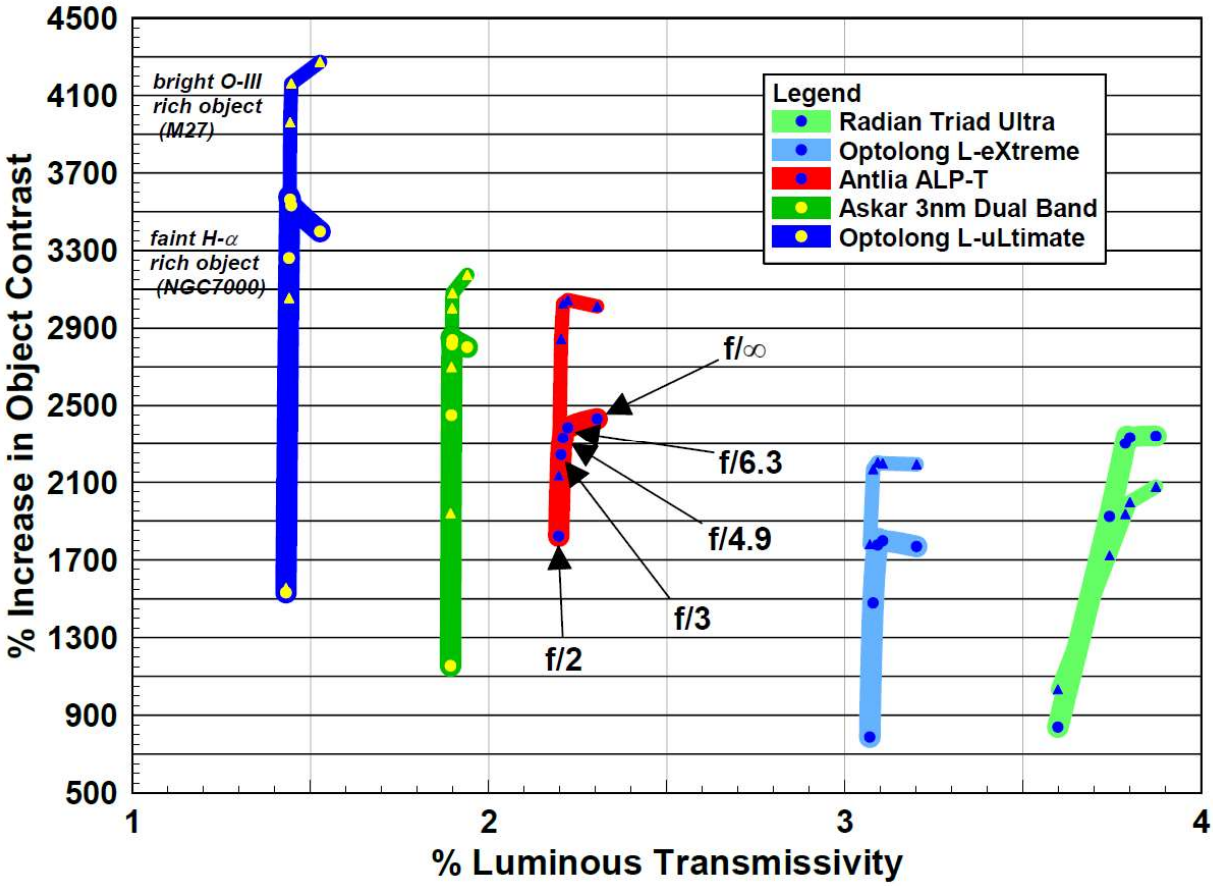


**Figure 8 Predicted Filter Performance: Back Illuminated OSC CMOS, Bortle 9+ Sky**

As expected, the predictions suggest that the narrower the filter's pass bands (and thus lower %LT), the larger the contrast increase. The exception being the Triad Ultra's performance on faint H-α rich nebula, which is predicted to be comparable to that of the 5nm wide ALP-T, presumably because of the presence of a pass band at H-β that adds to the total nebula emission passed by the filter. The Askar filter, with its pass bands measured at wider than 3nm, is

predicted to perform more similar to the ALP-T than the L-uLtimate. The L-uLtimate filter has the narrowest pass bands and therefore is predicted to deliver the largest increase in contrast.

The sensitivity of each filter to f-ratio is evident in the length of each line on the plot. As expected, the filters with the narrowest pass bands are most sensitive to f-ratio, that is they have the largest variation in performance with f-ratio. The predicted contrast increase of O-III rich targets for the two 3nm filters starts to steeply decline for f-ratios below f/6. On H-α rich targets the effect is delayed a bit, with the contrast increase not starting to steeply decline until f-ratios around f/4.5.

Another thing to note from Figure 8 is the trade-off between contrast increase and exposure time compared with the other filters under test. For example: the L-uLtimate filter is predicted to provide a contrast increase that is 96% larger than the L-eXtreme on faint H-α nebulae (3533% vs. 1798% @ f/6.3), but at the cost of 2.1x the exposure time (%LT of 1.45% vs. 3.11%). Before purchasing one of these new 3nm filters, it is important for the user to understand what the impact will be on the way they collect their image data.

**Results - Imaging:**
All image collection on a particular night was done within a one-hour time window. This process was repeated four times, each on a different deepsky target as described above. Images were generated by live stacking in Sharpcap, with a sufficient number of sub's captured in each case to generate a stack with either 5 or 10 minutes total exposure. Imaging results from the four sessions are provided below. The images presented are of the final stacks. All the images had their histograms adjusted in exactly the same way using Fitswork v4.47, a free FITS editing software, so that they provide as fair a visual comparison as possible. The imaging results are presented below both as an RGB image and as the red channel and green channel displayed separately so that the relative performance on O-III (green channel) and H-α (red channel) are easier to visualize.

Images from the first imaging session are shown in Figures 9 to 11, second imaging session Figures 12 to 14, third imaging session Figures 15 to 17, and the last imaging session Figures 18 to 20. In general, the differences visible between filters on the same target are very subtle. Only after close examination is it possible to identify features that are more prominent in one filter's image than another's. All the filters tested delivered images with good contrast and detail from my Bortle 9+ backyard. To be able to extract more quantitative observations it was required to do some image analysis using software tools.

*Triad Ultra (20 x 30s)*

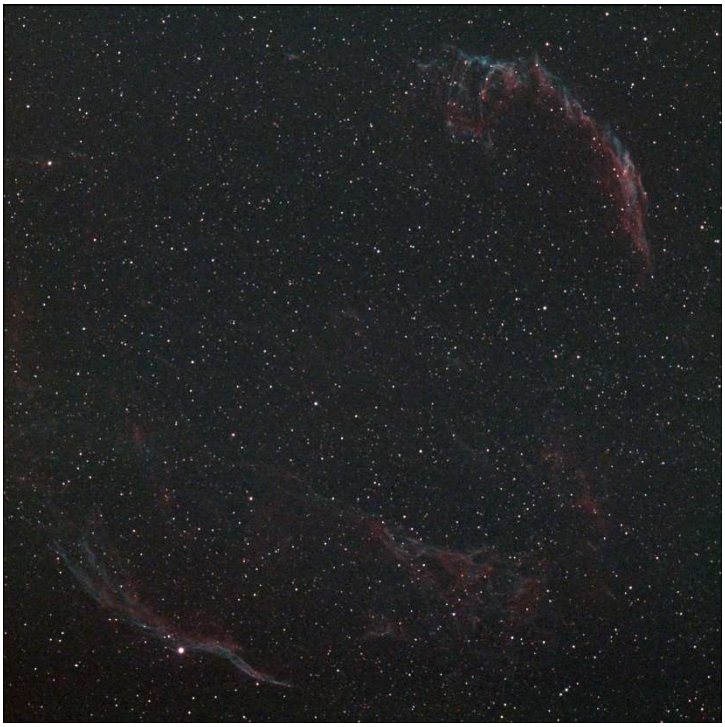

*L-eXtreme (15 x 40s)*

*ALP-T (12 x 50s)*

*L-uLtimate (10 x 60s)*

**Figure 9 Sept. 8th Imaging Results – FMA230, Cygnus Loop, RGB**

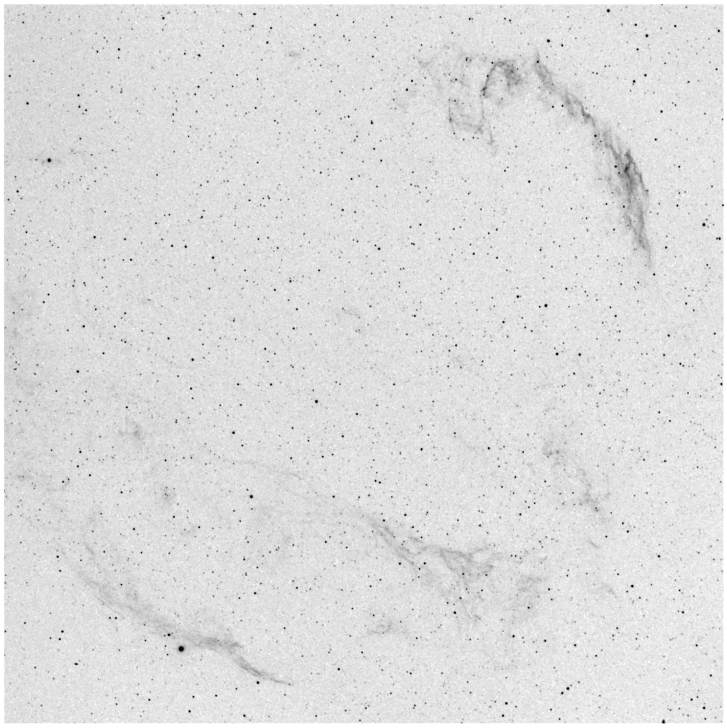

*Triad Ultra (20 x 30s)*

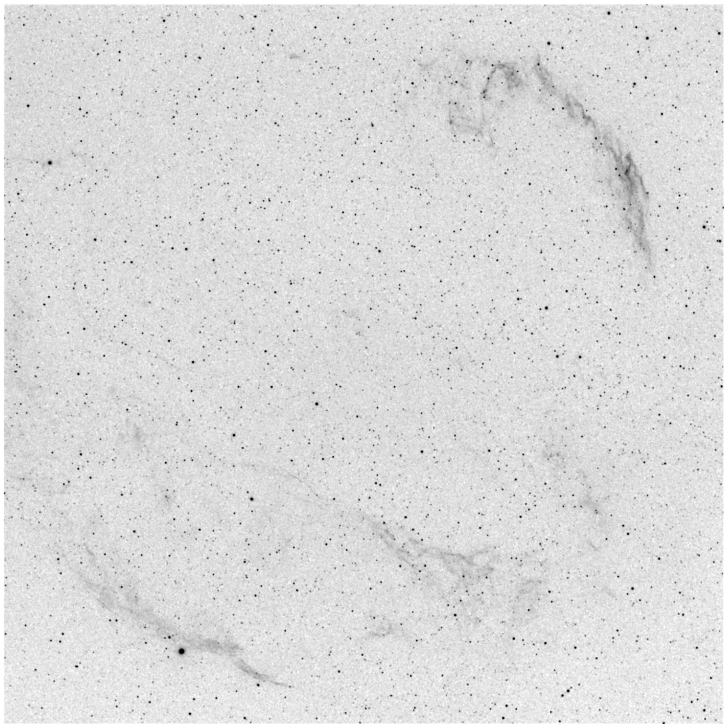

*L-eXtreme (15 x 40s)*

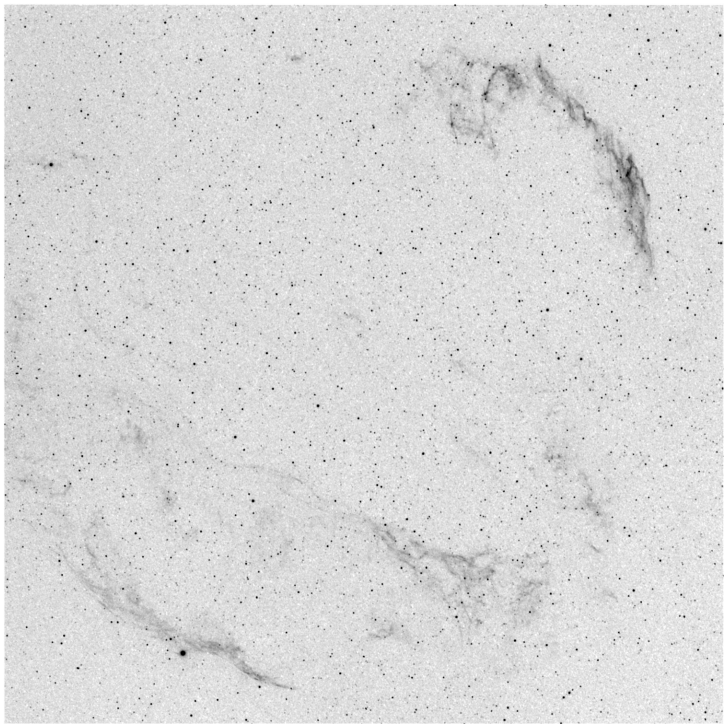

*ALP-T (12 x 50s)*

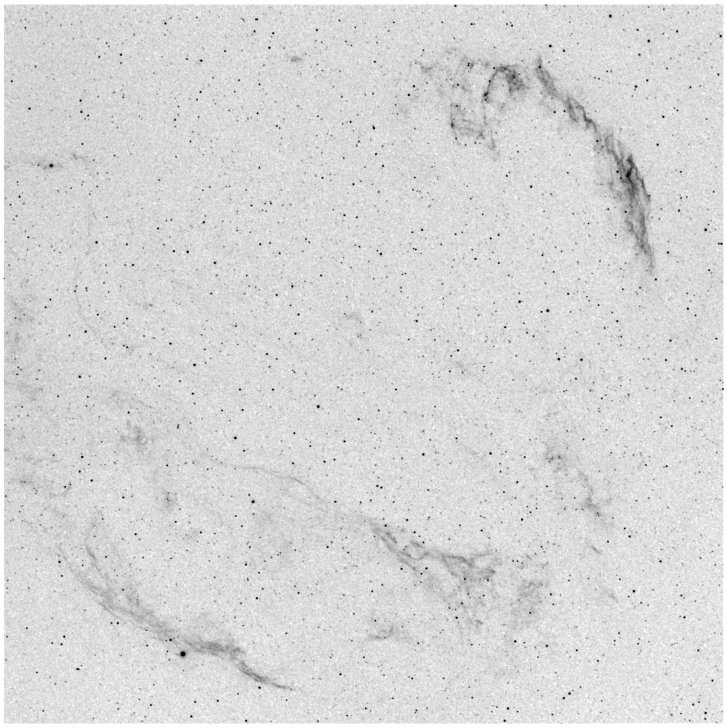

*L-uLtimate (10 x 60s)*

**Figure 10 Sept. 8th Imaging Results – FMA230, Cygnus Loop, Red Channel**

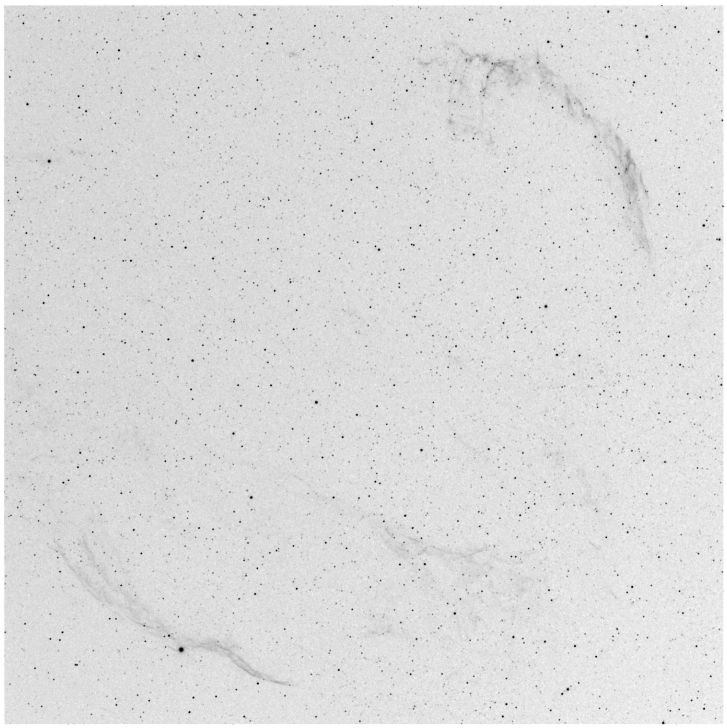

*Triad Ultra (20 x 30s)*

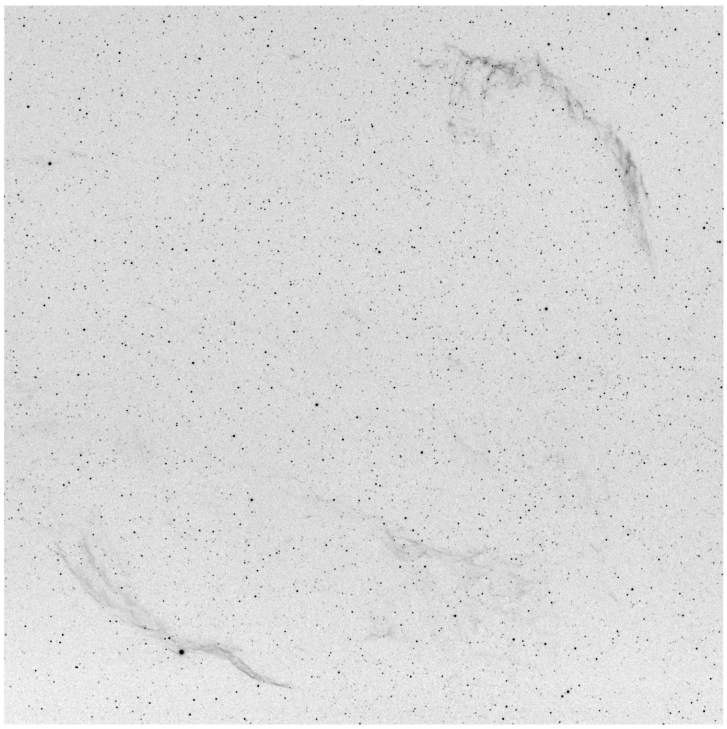

*L-eXtreme (15 x 40s)*

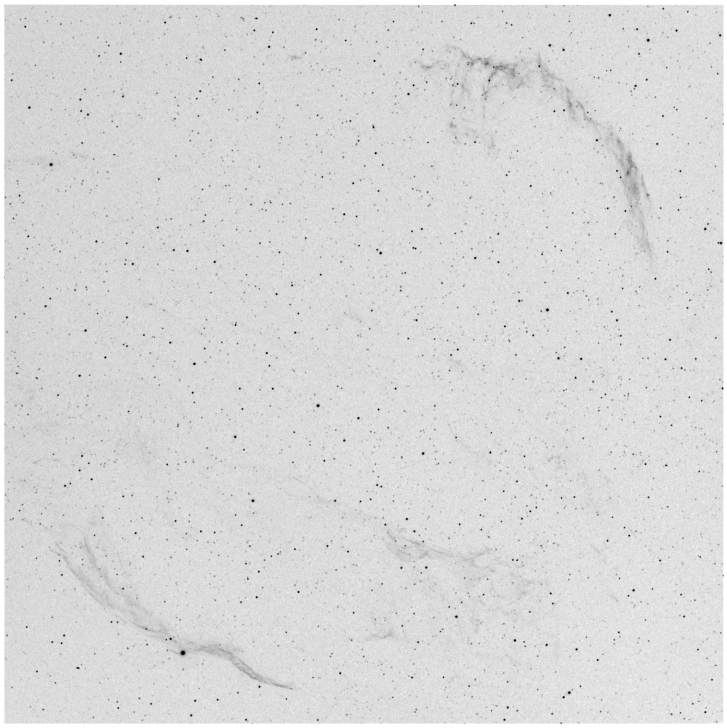

*ALP-T (12 x 50s)*

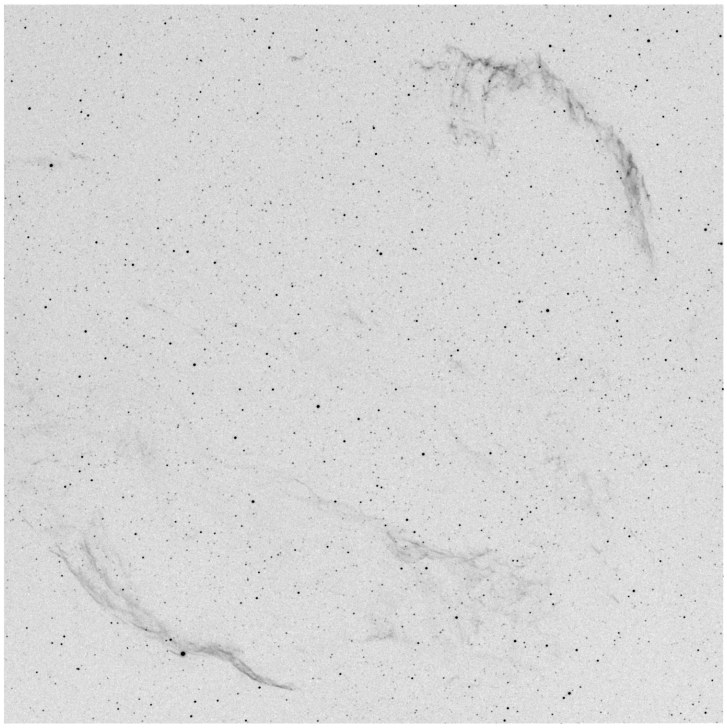

*L-uLtimate (10 x 60s)*

**Figure 11 Sept. 8th Imaging Results – FMA230, Cygnus Loop, Green Channel**

*Triad Ultra (10 x 30s)*

*L-eXtreme (8 x 40s)*

*ALP-T (6 x 50s)*

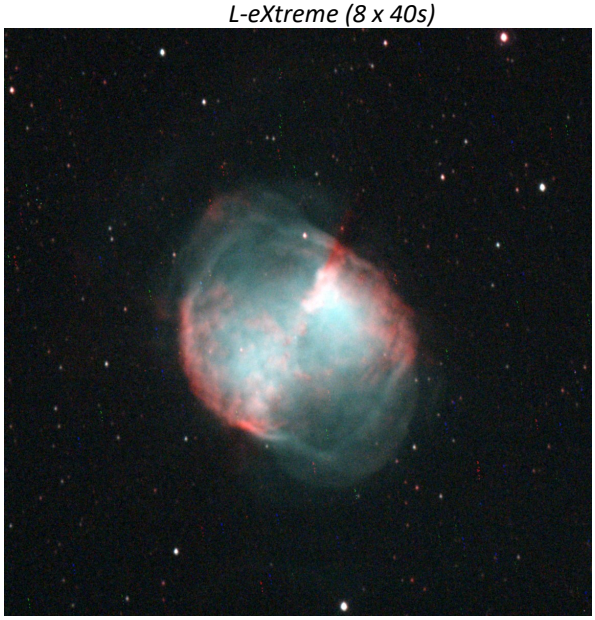

*L-uLtimate (5 x 60s)*

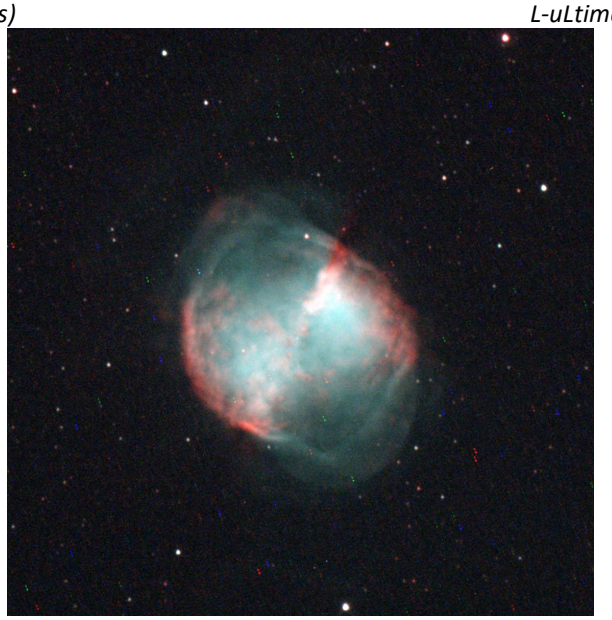

*L-uLtimate (10 x 30s)*

**Figure 12 Sept. 29th Imaging Results – VRC10, M27 Dumbbell Nebula, RGB**

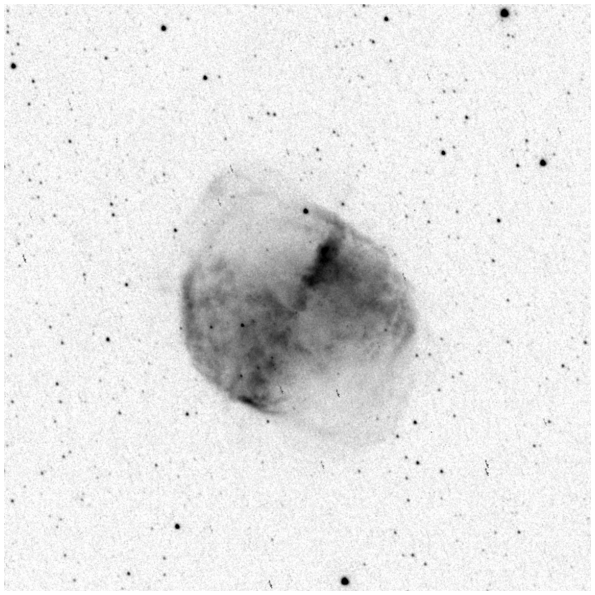

*Triad Ultra (10 x 30s)*

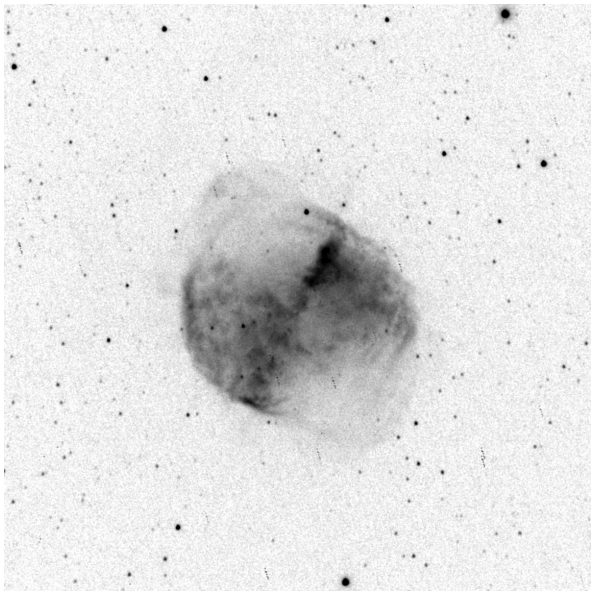

*L-eXtreme (8 x 40s)*

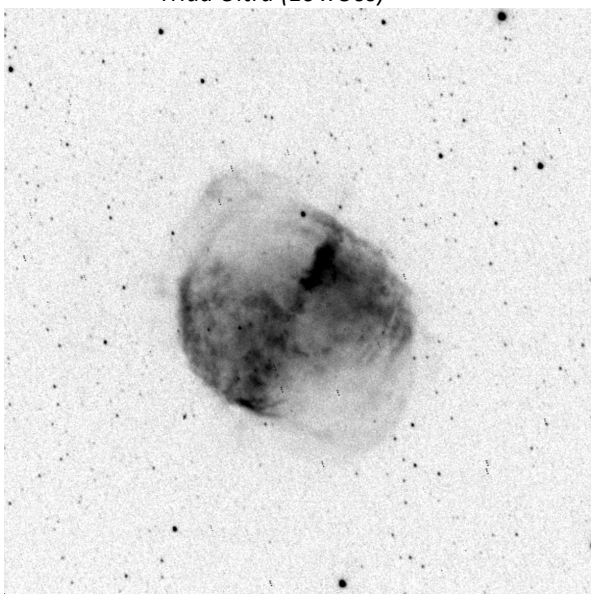

*ALP-T (6 x 50s)*

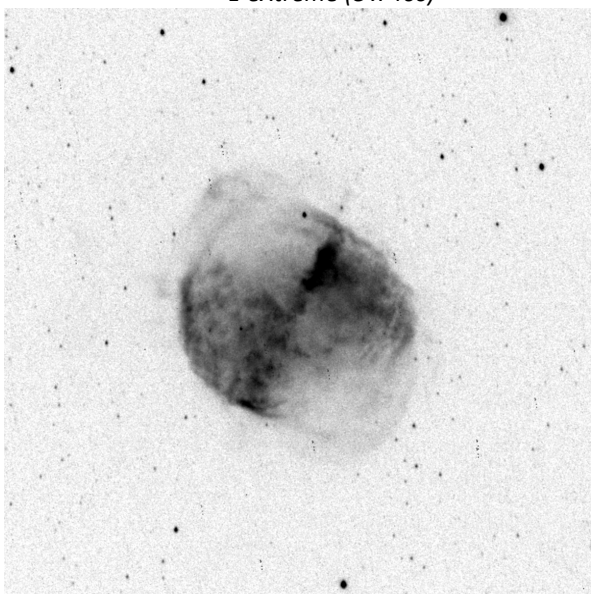

*L-uLtimate (5 x 60s)*

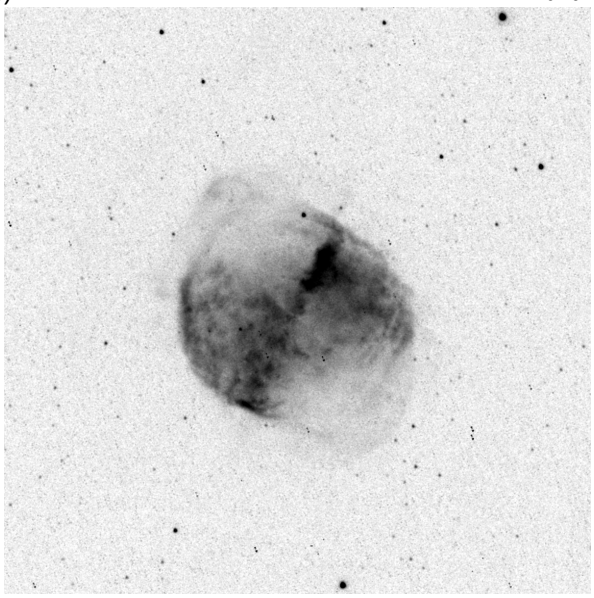

*L-uLtimate (10 x 30s)*

**Figure 13 Sept. 29th Imaging Results – VRC10, M27 Dumbbell Nebula, Red Channel**

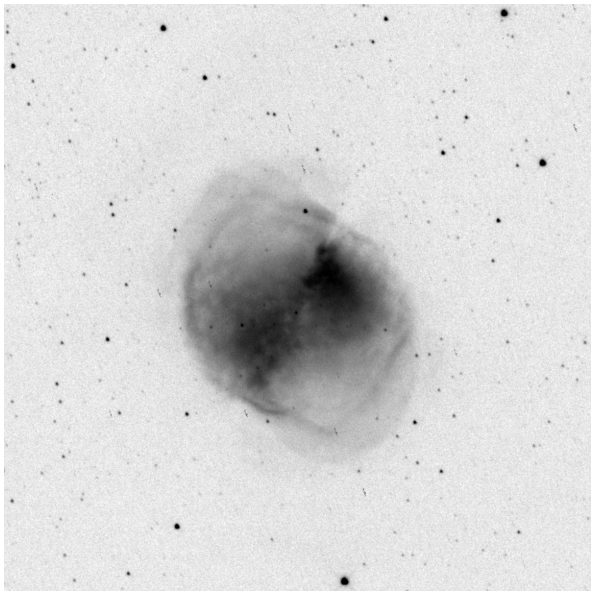

*Triad Ultra (10 x 30s)*

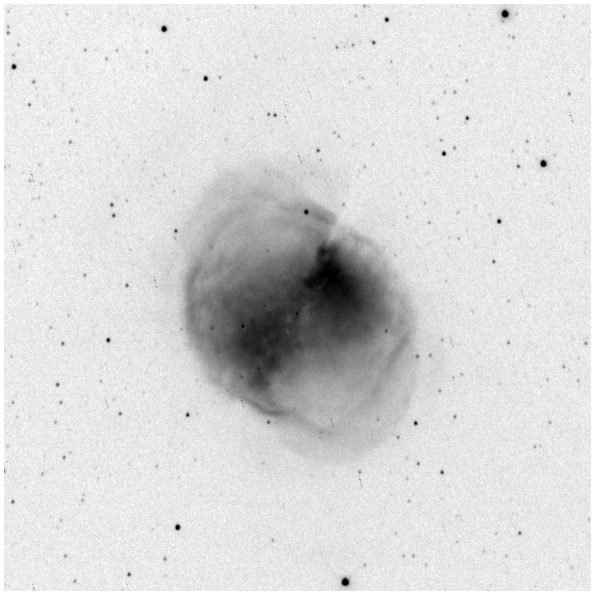

*L-eXtreme (8 x 40s)*

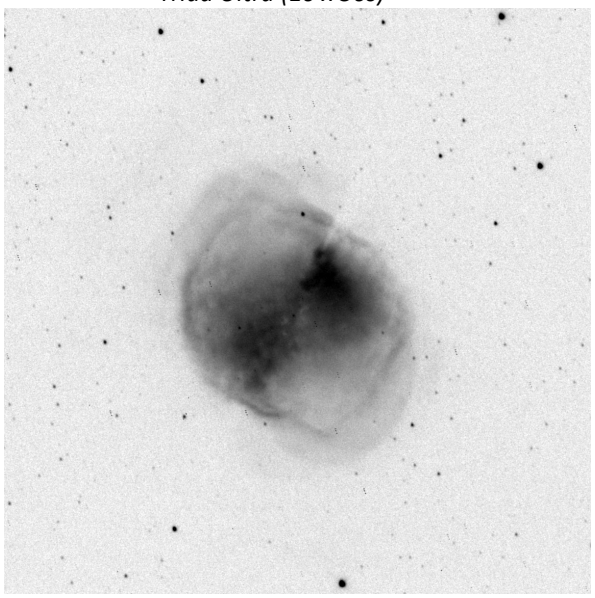

*ALP-T (6 x 50s)*

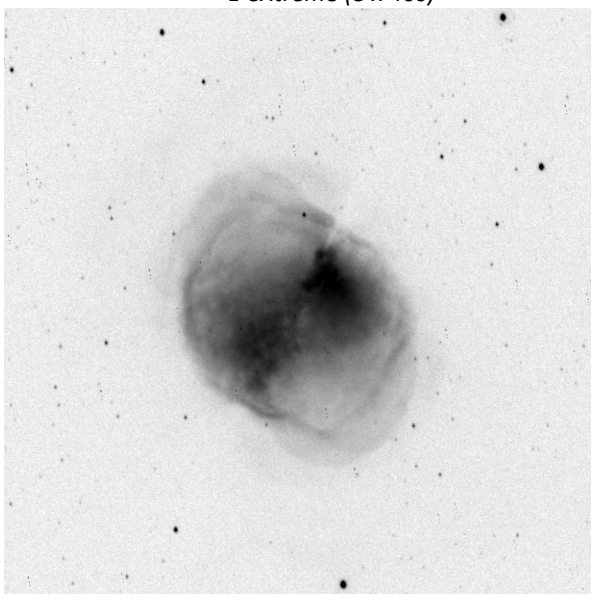

*L-uLtimate (5 x 60s)*

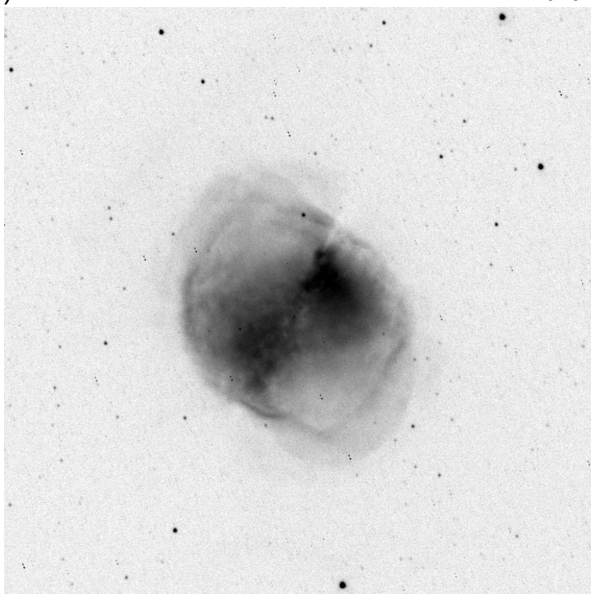

*L-uLtimate (10 x 30s)*

**Figure 14 Sept. 29th Imaging Results – VRC10, M27 Dumbbell Nebula, Green Channel**

*Triad Ultra (5 x 60s)*

*L-eXtreme (5 x 60s)*

*ALP-T (5 x 60s)*

*3nm Duo-Narrowband (5 x 60s)*

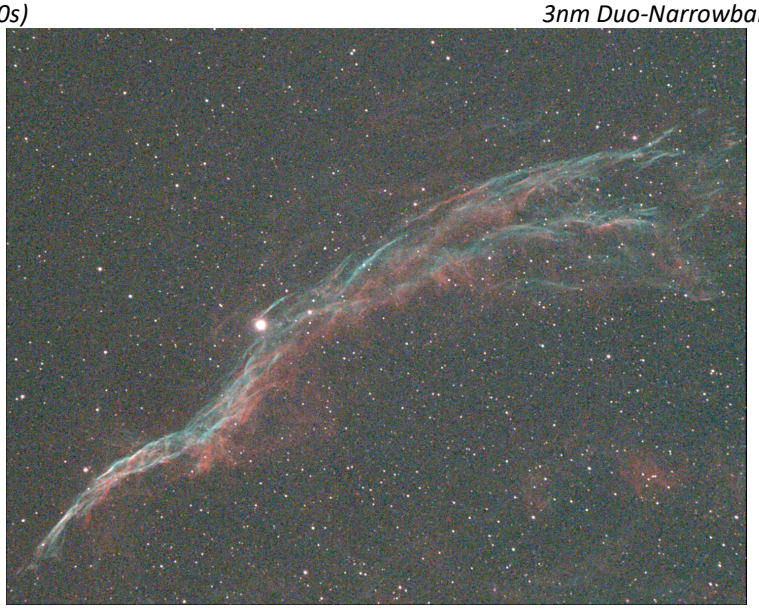

*L-uLtimate (5 x 60s)*

**Figure 15 Oct. 18th Imaging Results – FLT98, NGC6960 Western Veil Nebula, RGB**

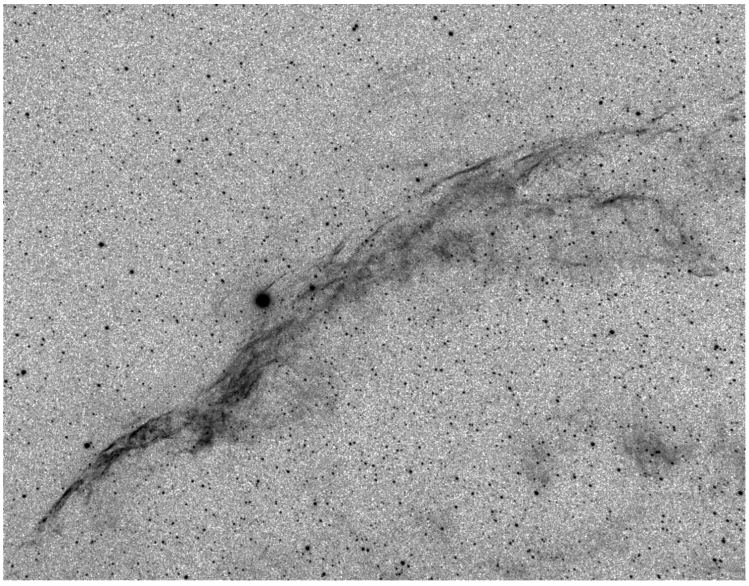

*Triad Ultra (5 x 60s)*

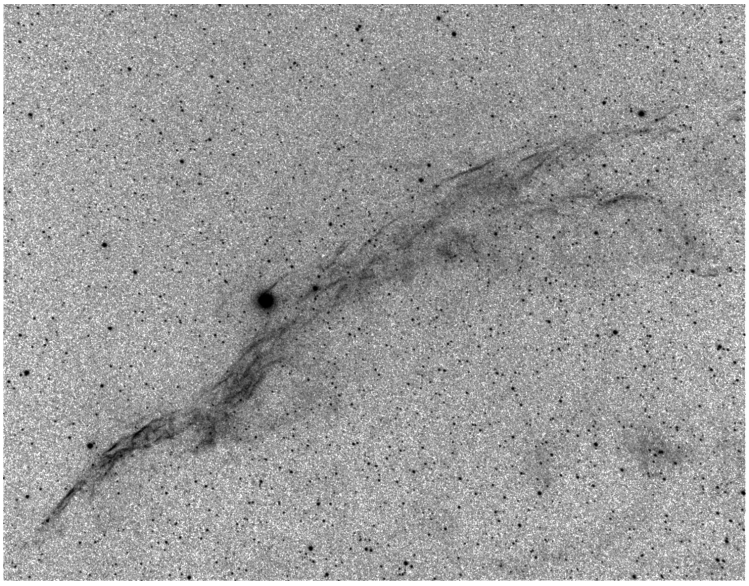

*L-eXtreme (5 x 60s)*

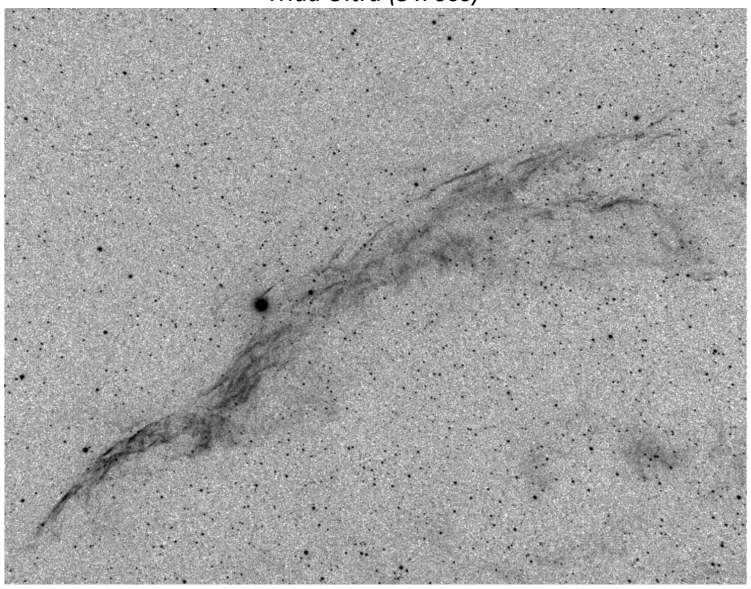

*ALP-T (5 x 60s)*

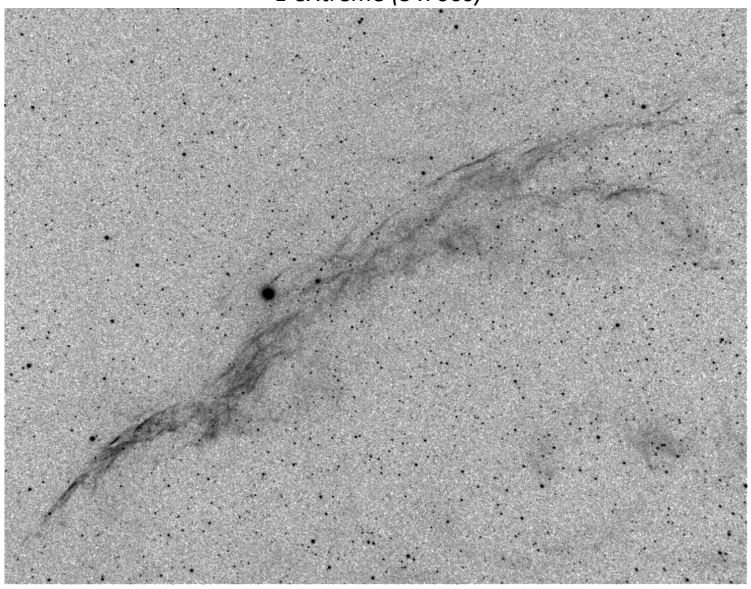

*3nm Duo-Narrowband (5 x 60s)*

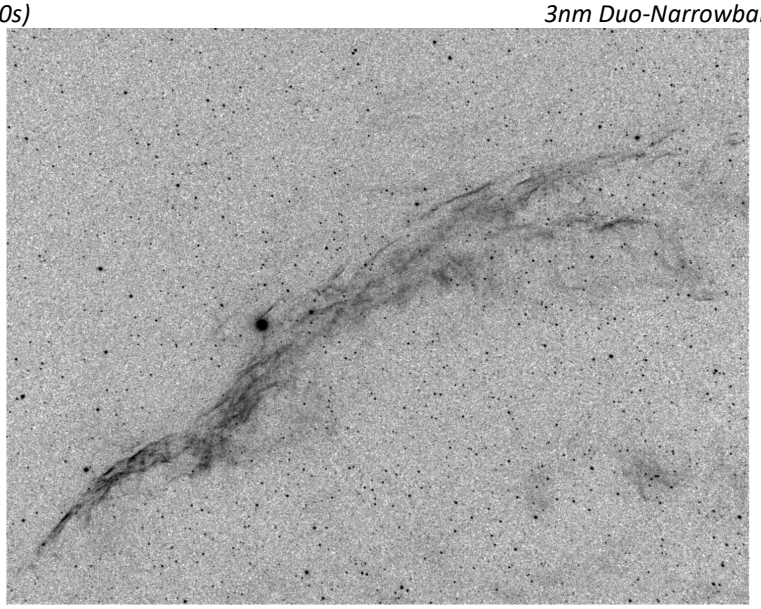

*L-uLtimate (5 x 60s)*

**Figure 16 Oct. 18th Imaging Results – FLT98, NGC6960 Western Veil Nebula, Red Channel**

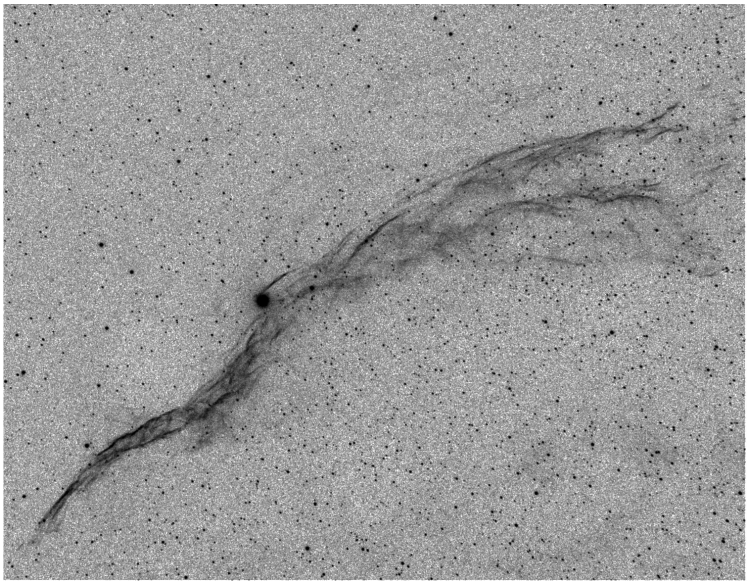

*Triad Ultra (5 x 60s)*

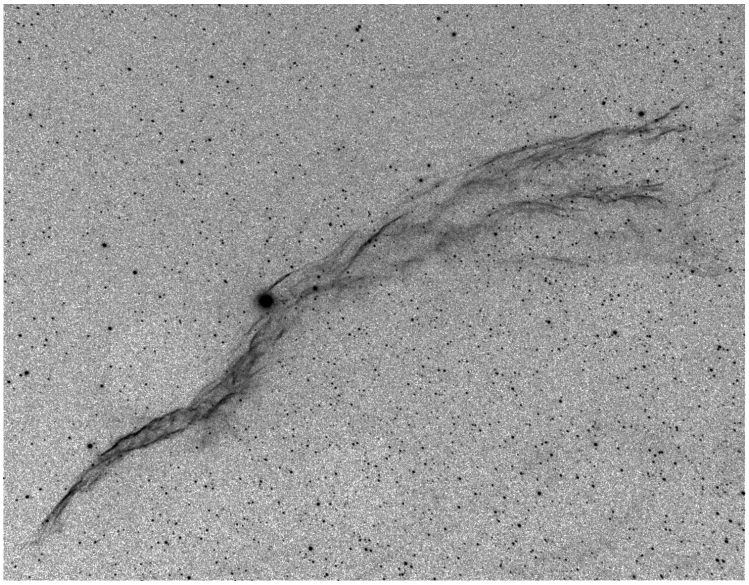

*L-eXtreme (5 x 60s)*

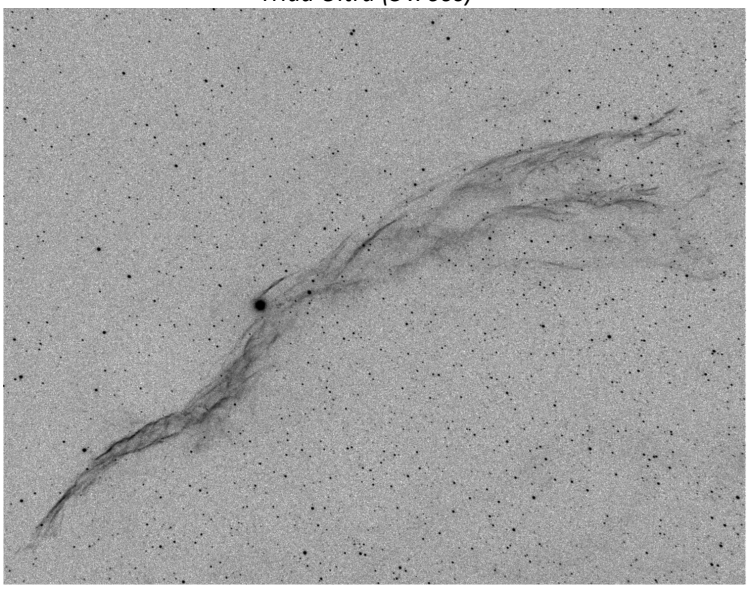

*ALP-T (5 x 60s)*

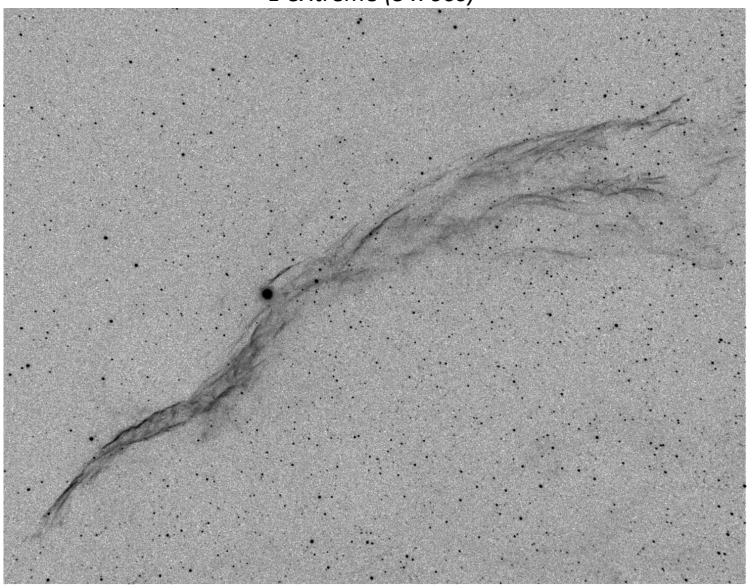

*3nm Duo-Narrowband (5 x 60s)*

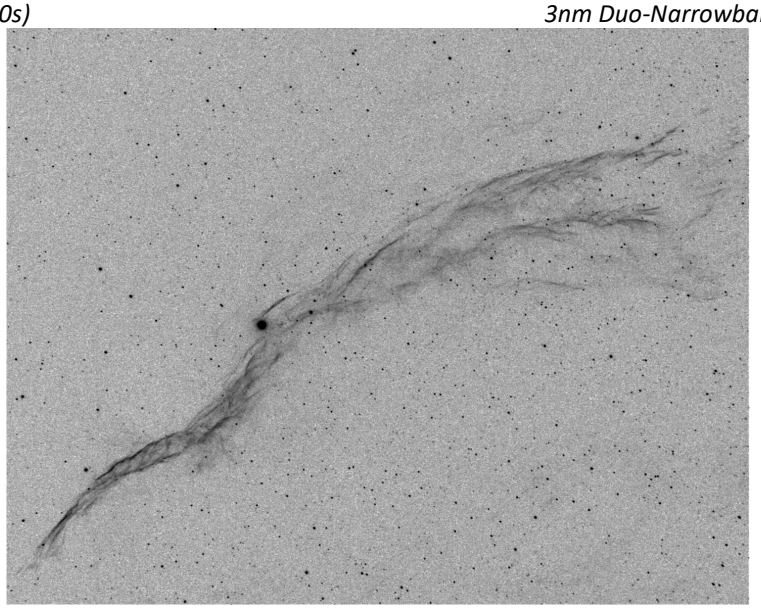

*L-uLtimate (5 x 60s)*

**Figure 17 Oct. 18th Imaging Results – FLT98, NGC6960 Western Veil Nebula, Green Channel**

*Triad Ultra (10 x 30s)*

*L-eXtreme (8 x 40s)*

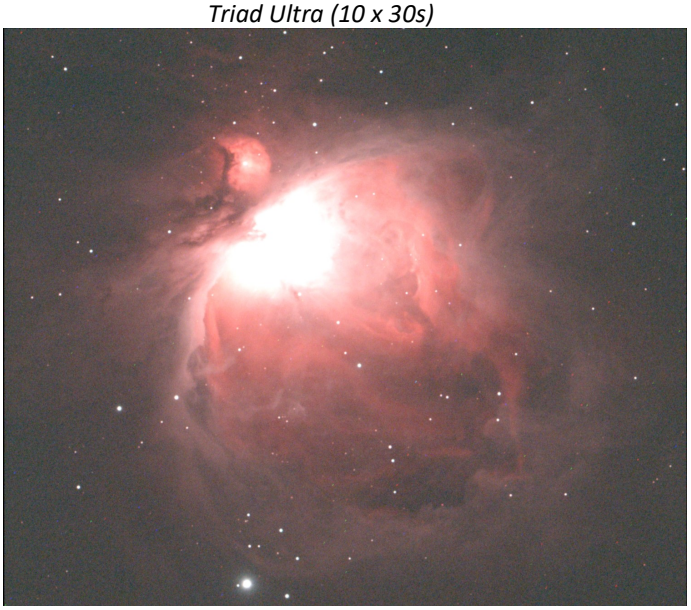

*ALP-T (6 x 50s)*

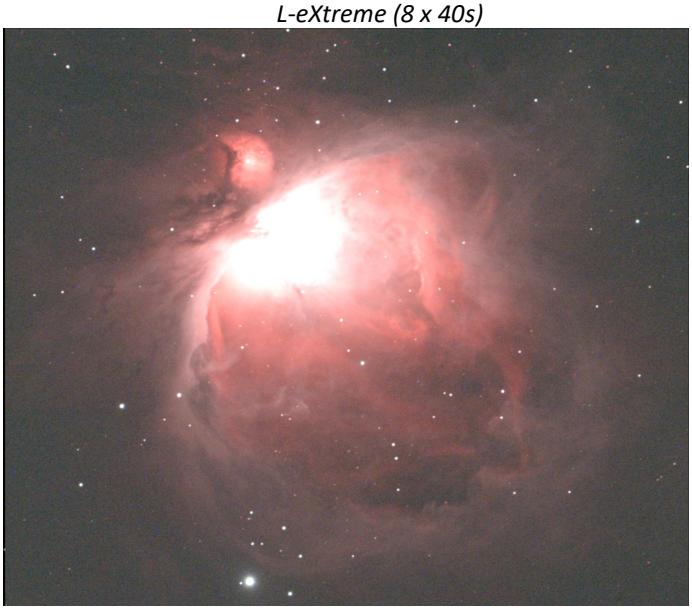

*3nm Duo-Narrowband (6 x 55s)*

*L-uLtimate (5 x 60s)*

**Figure 18 Oct. 22nd Imaging Results – FLT98, M42 Orion Nebula, RGB**

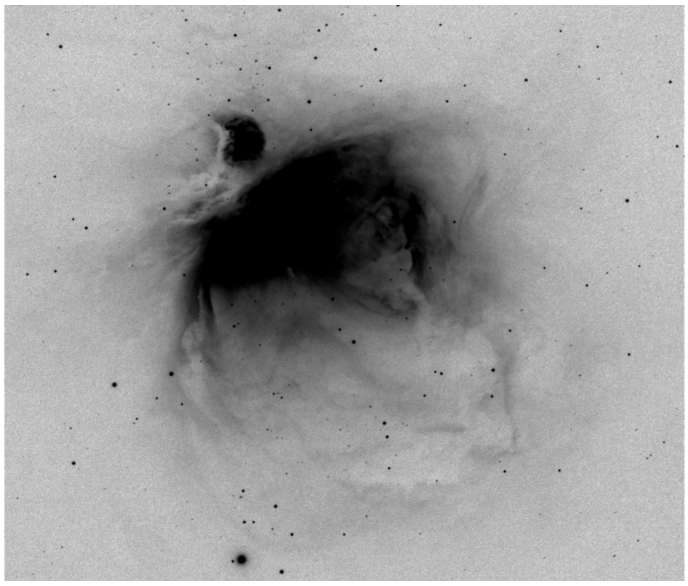

*Triad Ultra (10 x 30s)*

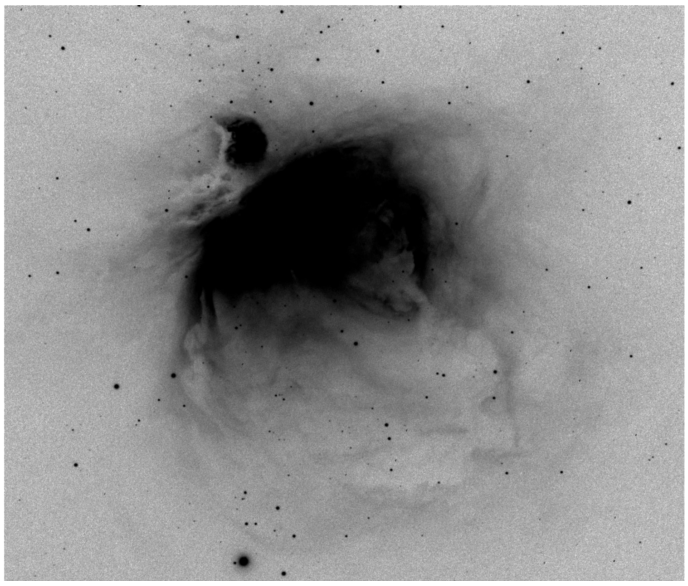

*L-eXtreme (8 x 40s)*

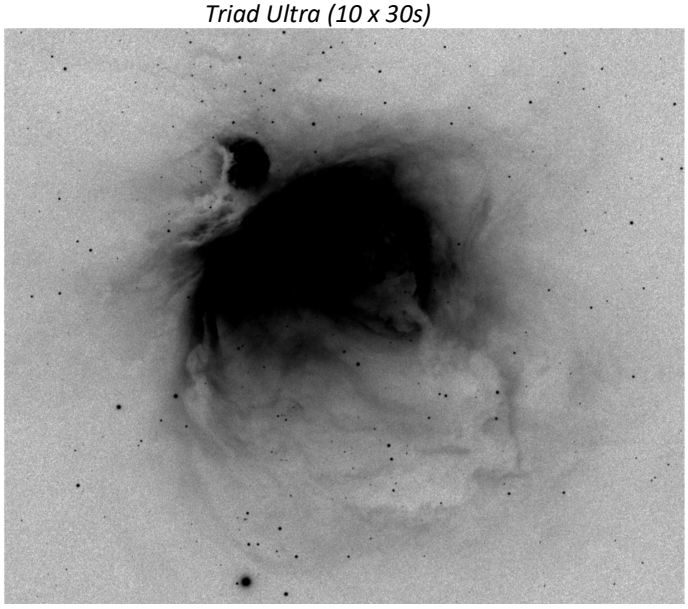

*ALP-T (6 x 50s)*

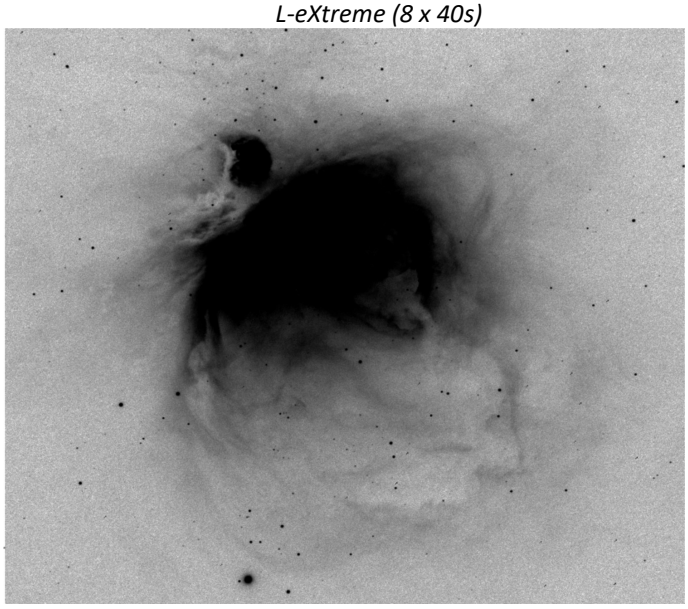

*3nm Duo-Narrowband (6 x 55s)*

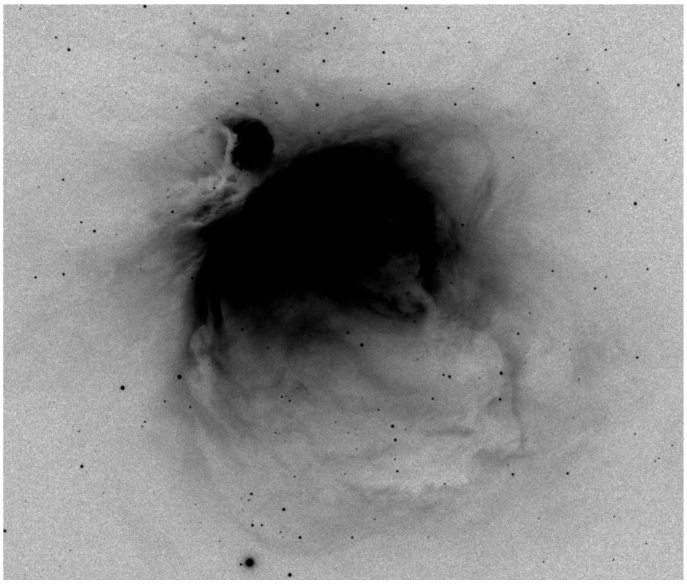

*L-uLtimate (5 x 60s)*

**Figure 19 Oct. 22nd Imaging Results – FLT98, M42 Orion Nebula, Red Channel**

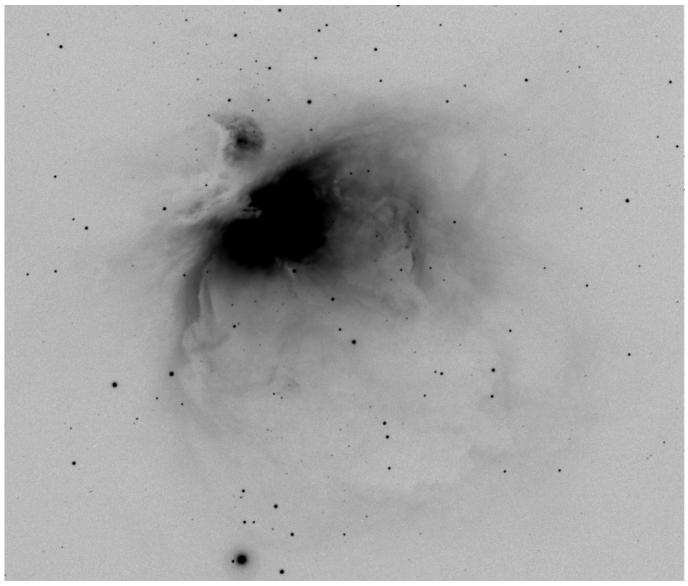

*Triad Ultra (10 x 30s)*

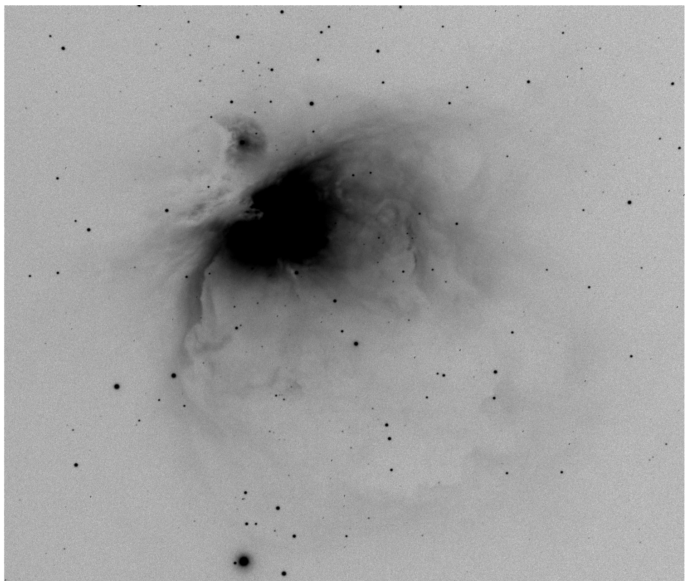

*L-eXtreme (8 x 40s)*

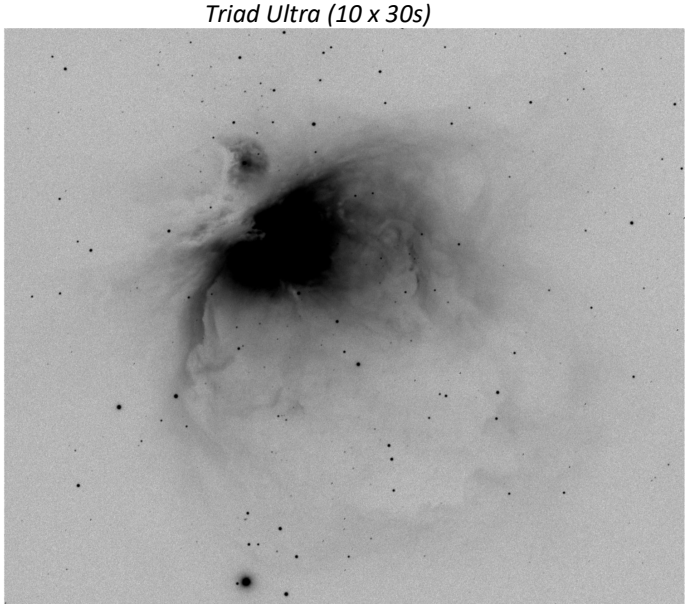

*ALP-T (6 x 50s)*

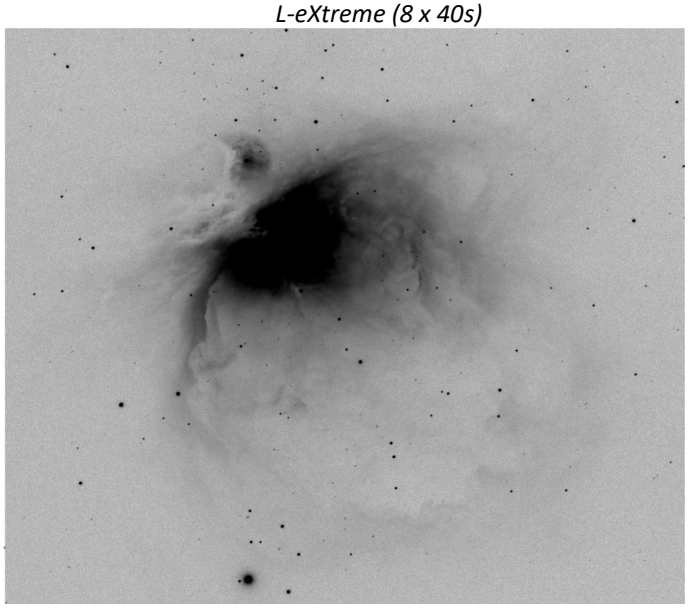

*3nm Duo-Narrowband (6 x 55s)*

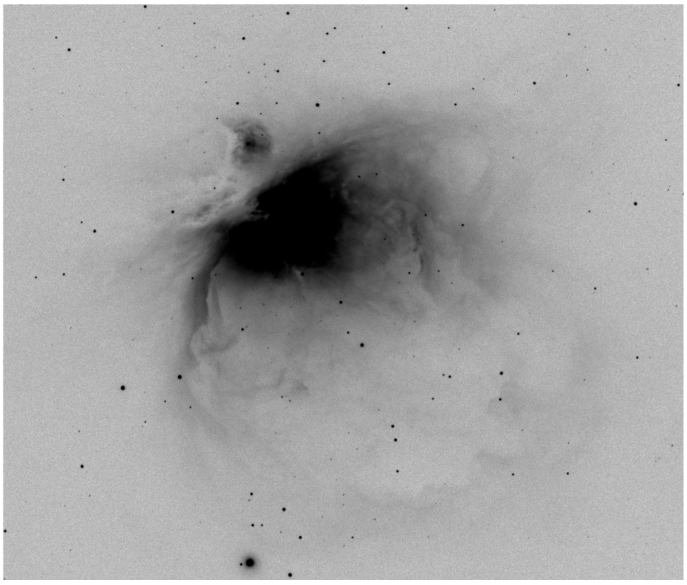

*L-uLtimate (5 x 60s)*

**Figure 20 Oct. 22nd Imaging Results – FLT98, M42 Orion Nebula, Green Channel**

Using the captured image data I was able to directly measure the contrast increase delivered by each filter, putting a number to what was already observed qualitatively from the images in Figures 9 through 20. This was accomplished by using AstroImageJ to measure the average luminance from two common areas in the images: a dark background area, and a bright nebulous area. The particular areas used are illustrated in Figure 21 (red box for nebulosity, blue box for background), with these same areas used for all the images from the various filters. Measurements of luminance average and standard deviation were taken from the original unedited FITS files in each colour channel. Contrast increase was calculated from the measured luminance values using the following equations:

Measured Contrast = [measured nebula luminance – measured background luminance] ÷ measured background luminance

% Contrast Increase = [contrast w/filter – contrast w/out filter] ÷ contrast w/out filter x 100

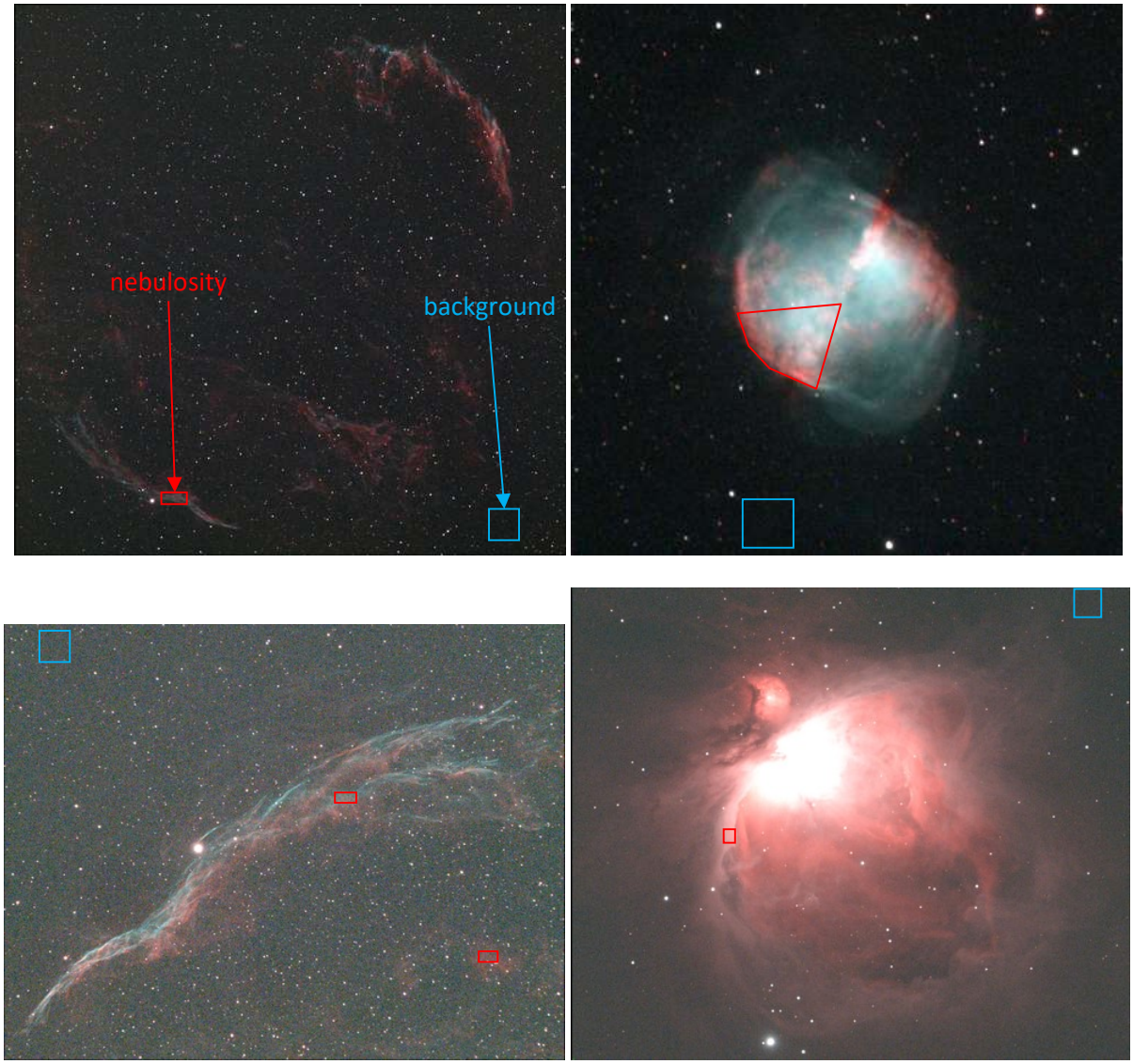


**Figure 21 Areas Used for Image Analyses**

The resulting contrast increase measurements are plotted in Figure 22, along with the corresponding prediction for each filter. The absolute value of the measurements are consistently below the predictions, however the relative performance of one filter to the other matches the prediction very well. There are a number of reasons why the magnitude of the measurements might not match the predictions, the most important reason being the sky conditions during the imaging sessions (i.e. transparency) were likely worse than assumed in the prediction calculations.

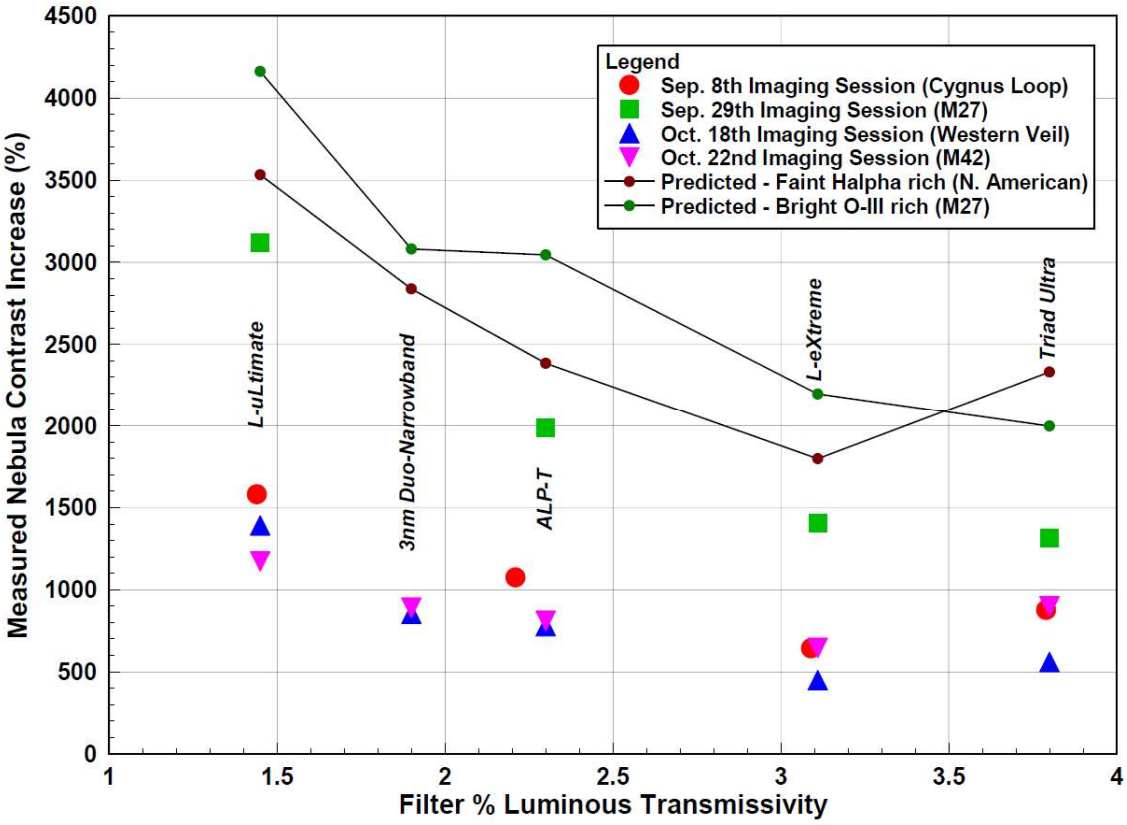


**Figure 22 Measured Nebula Contrast Increase, M8 Images**

The measurement of luminance from the images also allowed me to calculate the impact of each filter on exposure time. Figure 23 plots the %LT of each filter, as calculated from the spectrometer data, against the exposure (i.e. overall brightness) of the recorded images from each session divided by sub-exposure time. The black diagonal line in the plot represents perfect correlation; the closer the measured points are to this line the better an estimate of relative exposure the calculated %LT is. Based on the results, %LT is reasonably well correlated with the actual measured relative exposure time.

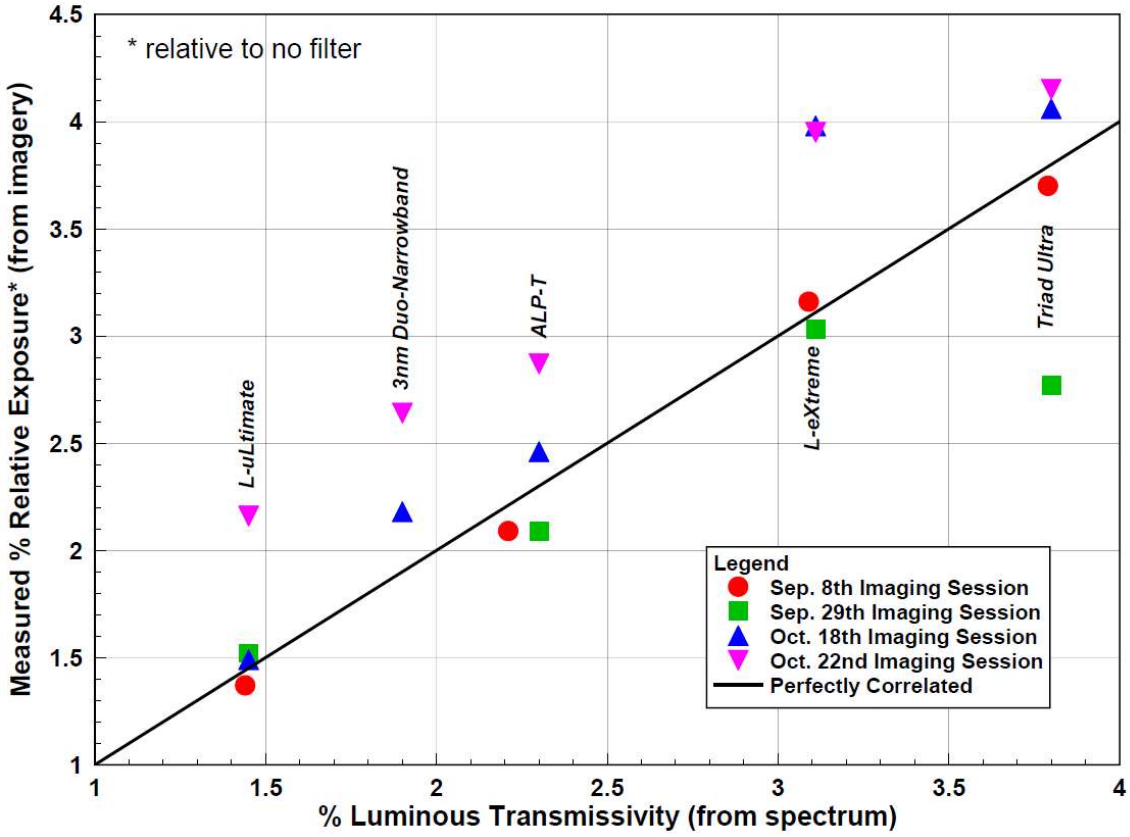


**Figure 23 Measured Nebula Contrast Increase, M8 Images**

Finally, the measurements of luminance from the images allowed me to evaluate signal-to-noise ratio (SNR). When I extracted the average luminance values from each image in AstroImageJ, I also recorded the standard deviation (σ). This allowed me to calculate the SNR achieved by each filter using the following equation:

SNR = (measured nebula luminance – measured background luminance) ÷ measured nebula σ

The SNR measurement results, from the 5 minute stacked images collected during imaging session #3, are shown in Table 2. As expected, there is an increase in the SNR of the nebula the narrower the filter used, with the L-uLtimate filter delivering the best SNR of the filters tested.

| Filter | %LT @ f/6.3 | SNR (5x60s) | $USD/ SNR |
|---|---|---|---|
| No Filter | 100% | 0.40* | - |
| Radian Triad Ultra | 3.80% | 2.65 | $406 |
| Optolong L-eXtreme | 3.11% | 2.51 | $123 |
| Antlia ALP-T | 2.22% | 2.77 | $137 |
| Askar Colour Magic 3nm Duo-Narrowband | 1.90% | 3.02 | $178 |
| Optolong L-uLtimate | 1.45% | 3.61 | $108 |

**Way over exposed w/ 60s sub-exposure, so used 300x1s instead*

**Table 2 Measured Nebula SNR, Image Session #3**

**Star Halos:**
A performance parameter that I have not devoted much attention to in the past, but that has been brought to my attention as an important detail to astrophotographers, is the extent to which a filter displays halos around bright stars. My investigation of this topic has spun-off an entirely new and rather elaborate test program, the results of which I hope to report on soon. In the meantime, Figure 24 presents crops around a particularly bright star from the images collected during my third and fourth imaging sessions. The stars in particular are: 52 Cygni from session #3 (+4.22 magnitude, surface temperature 4677K), and ι-Orionis (Nair al Saif) from session #4 (+2.77 magnitude, surface temperature 32,500K). Although no discernable halos were visible around 52 Cygni, there were around the much hotter star ι-Orionis. The imaging results suggest that the L-uLtimate filter displays a very subdued but still visible halo around bright hot stars, while the Askar filter displays virtually no halo. The worst halo was displayed by the Triad Ultra filter, the halo being larger and brighter than that presented by any of the other filters tested.

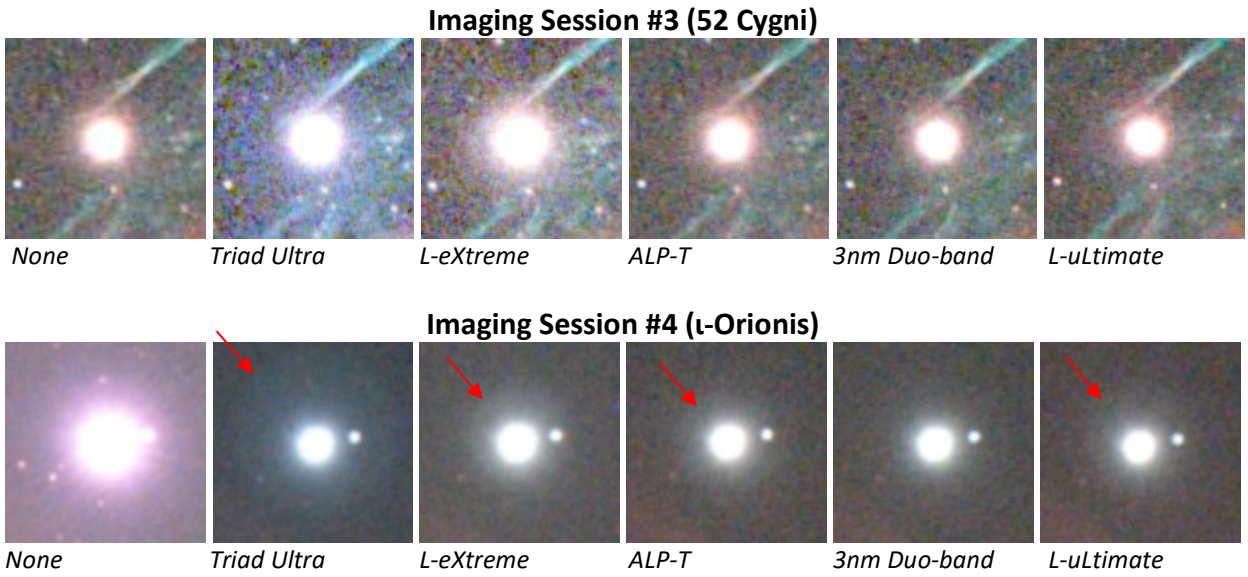


**Figure 24 Crop of Bright Stars From Imaging Sessions #3 & #4 (Halos highlighted w/ arrows)**

**Conclusions:**
Based on the results of the testing described above, I have made the following conclusions:

1. Of the two 3nm filters tested, only the L-uLtimate had measured properties that were fully consistent with the manufacturer's specifications. The Askar filter was measured to have peak transmission values consistent with manufacturer's specifications, but the FWHM for the filter's two pass bands were measured to be significantly wider than spec.
2. The L-uLtimate filter, having the narrowest pass bands of the filters tested, delivered the largest increase in nebula contrast. This was demonstrated both by analysis (spectrums) and by test (imaging). The L-uLtimate also delivered the best SNR for the same exposure time of all the filters tested. The Askar filter was the second highest performer, delivering a contrast increase and SNR slightly better than the ALP-T.

3. To realize the full advantage of the narrower filters requires the use of longer sub-exposure times. The extent to which the filter affects sub-exposure time is proportional to the %LT values calculated for each filter from their measured spectrums.
4. In terms of cost-performance benefit, the L-uLtimate filter has the best $USD per SNR at $108. The Askar filter is not priced competitively relative to the other filters (excluding the Triad Ultra), having a $USD per SNR of $178.
5. The L-uLtimate filter produces very subdued but still visible halos around hot bright stars. The Askar filter does not seem to produce any discernable halos around stars.

If you have any questions, please feel free to contact me.

Cheers!

Jim Thompson
(top-jimmy@rogers.com)